AFOSR-TR- 90-0343

Microwave Laboratory Report No. 90-P-1

Monolithic Phase Shifter Study

D. P. Neikirk and T. Itoh
University of Texas at Austin
Department of Electrical and Computer Engineering
Austin, TX 78712

February 15, 1990

Final Technical Report for the Period November 1985- October 1988 for
AFOSR Grant No. AFOSR-86-0036

Prepared For:

AIR FORCE OFFICE OF SCIENTIFIC RESEARCH
Bolling Air Force Base, DC 20332-6448

Microwave Laboratory Report No. 90-P-1

Monolithic Phase Shifter Study

D. P. Neikirk and T. Itoh
University of Texas at Austin
Department of Electrical and Computer Engineering
Austin, TX 78712

February 15, 1990

Final Technical Report for the Period November 1985- October 1988 for
AFOSR Grant No. AFOSR-86-0036

Prepared For:

AIR FORCE OFFICE OF SCIENTIFIC RESEARCH
Bolling Air Force Base, DC 20332-6448

SECURITY CLASSIFICATION OF THIS PAGE

REPORT DOCUMENTATION PAGE

Form Approved OMB No. 0704-0188

1a. REPORT SECURITY CLASSIFICATION UNCLASSIFIED	1b. RESTRICTIVE MARKINGS
2a. SECURITY CLASSIFICATION AUTHORITY	3. DISTRIBUTION/AVAILABILITY OF REPORT Unlimited
2b. DECLASSIFICATION/DOWNGRADING SCHEDULE	
4. PERFORMING ORGANIZATION REPORT NUMBER(S) Microwave Laboratory Reprt No. 90-P-1	5. MONITORING ORGANIZATION REPORT NUMBER(S)
6a. NAME OF PERFORMING ORGANIZATION The University of Texas; 6b. OFFICE SYMBOL (If applicable)	7a. NAME OF MONITORING ORGANIZATION AFOSR/NE
6c. ADDRESS (City, State, and ZIP Code) Dept. of Electrical & Computer Engineering, The University of Texas, Austin, TX 78712	7b. ADDRESS (City, State, and ZIP Code) Bldg 410, Bolling AFB, DC 20332-6448
8a. NAME OF FUNDING/SPONSORING ORGANIZATION AFOSR/NE; 8b. OFFICE SYMBOL (If applicable) NE	9. PROCUREMENT INSTRUMENT IDENTIFICATION NUMBER AFOSR-86-0036
8c. ADDRESS (City, State, and ZIP Code) Building 410, Bolling AFB, DC 20332-6448	10. SOURCE OF FUNDING NUMBERS: PROGRAM ELEMENT NO. 61102F; PROJECT NO. 2305; TASK NO C 1; WORK UNIT ACCESSION NO

11. TITLE (Include Security Classification)
Monolithic Phase Shifter Study

12. PERSONAL AUTHOR(S)
D. P. Neikirk and T. Itoh

13a. TYPE OF REPORT	13b. TIME COVERED	14. DATE OF REPORT (Year, Month, Day)	15. PAGE COUNT
Final Technical Rpt.	FROM Nov. 85 TO Oct. 88	1990, Feb. 15	53

16. SUPPLEMENTARY NOTATION

17. COSATI CODES			18. SUBJECT TERMS (Continue on reverse if necessary and identify by block number)
FIELD	GROUP	SUB-GROUP	coplaner waveguide, phase-shifter, optically-controlled

19. ABSTRACT (Continue on reverse if necessary and identify by block number)

Modeling and testing of monolithic coplanar waveguide (CPW) phase shifters using both optical and Schottky-contact control techniques have been performed. Simulation work on a periodically illuminated structure has been completed, showing that some improvement in performance may be possible, although with a reduction in frequency bandwidth. CPW transmission lines have been fabricated on semi-insulating GaAs, on lightly and heavily doped epi GaAs, and on an AlGaAs/GaAs heterostructure, and electrical characterization has been performed. Both Schottky-bias controlled and optically controlled phase shift has been obtained with the devices. A new control mechanism, using constant D.C. bias while using optical control has also been developed, which has yielded the best experimental performance to date for a distributed CPW phase shifter.

20. DISTRIBUTION/AVAILABILITY OF ABSTRACT ☒ UNCLASSIFIED/UNLIMITED ☐ SAME AS RPT. ☐ DTIC USERS	21. ABSTRACT SECURITY CLASSIFICATION Unclassified
22a. NAME OF RESPONSIBLE INDIVIDUAL ~~D. P. Neikirk~~ Dr Wittmann	22b. TELEPHONE (Include Area Code) ~~(512) 471-4669~~ 202-767-4984; 22c. OFFICE SYMBOL NE

DD Form 1473, JUN 86 Previous editions are obsolete. SECURITY CLASSIFICATION OF THIS PAGE

I. Summary

Modeling and testing of monolithic coplanar waveguide (CPW) phase shifters using both optical and Schottky-contact control techniques have been performed. Simulation work on a periodically illuminated structure has been completed, showing that some improvement in performance may be possible, although with a reduction in frequency bandwidth. CPW transmission lines have been fabricated on semi-insulating GaAs, on lightly and heavily doped epi GaAs, and on an AlGaAs/GaAs heterostructure, and electrical characterization has been performed. Both Schottky-bias controlled and optically controlled phase shift has been obtained with the devices. A new control mechanism, using constant D.C. bias while using optical control has also been developed, which has yielded the best experimental performance to date for a distributed CPW phase shifter.

II. Objectives and Status of Research

As discussed in our original proposal "Monolithic Phase Shifter Study," the objective of this work is to model, construct, and test prototype planar waveguide structures that could be used in monolithic millimeter-wave phase shifters. The following are the major accomplishments achieved under the sponsorship of this grant:

Theoretical Studies:

i) The basic control mechanisms for Schottky-contacted and optically-illuminated phase shifters have been elucidated. By means of relatively simple models, the essential requirements on conductivity and frequency have been identified. The CW optical intensities necessary for optically-controlled devices have been calculated including the effects of carrier diffusion and background doping;

ii) In order to better model the characteristics of coplanar waveguide (CPW) phase shifters, new numerical techniques have been developed to calculate the propagation characteristics of CPW's on substrates with non-uniform dielectric properties transverse to the guide;

iii) Theoretical analysis of wave propagation in a CPW with periodic optically-induced lossy patches has been performed. Such a device may provide better performance than the uniformly illuminated phase shifter.

Experimental Studies:

i) Several prototype CPW phase shifters have been fabricated on semi-insulating, lightly doped epi, heavily doped epi, and heterostructure substrates, and D.C., low frequency, and R.F. testing has been performed. Schottky bias-induced phase shift has been characterized, as well as optically induced phase shift. A new control mechanism based on the use of constant D.C. bias with variable optical illumination has been identified, and devices using this mechanism characterized;

ii) Prototype applications such as optically tunable resonators have been fabricated, and preliminary testing initiated.

The following discussion presents both background on phase shifters and a summary of work performed under the sponsorship of this grant.

III. Introduction and Background

In 1965 Hyltin [1] suggested that microstrip transmission lines could be fabricated on the same substrate as microwave devices to serve as interconnects, thus eliminating the need for hybrid circuits that give rise to parasitic inductances and capacitances. Subsequent theoretical studies showed that when these lines are fabricated on multi-layered semiconductor substrates (such as silicon dioxide (SiO_2) on silicon (Si) or aluminium gallium arsenide ($Al_xGa_{1-x}As$) on gallium arsenide (GaAs)), the lines could support three different characteristic modes of propagation [2, 3]. These studies showed that the occurrence of the different modes at a particular frequency is a function of the resistivity and the thickness of the layers of the substrate, as well as the dimensions of the transmission line. These modes are generally referred to as the skin-effect mode, the slow-wave (SW) mode, and the lossy dielectric mode. One of the more interesting applications of these phenomena is their use in distributed phase shifters, realized by controlling slow-wave propagation on layered semiconductor substrates.

In 1971 Hasegawa et al. [4] experimentally verified the existence of these modes for a microstrip on an SiO_2-Si substrate, over a wide range of substrate resistivity, dielectric thickness and microstrip width. The occurrence of the various modes was attributed to a Maxwell-Wagner effect that modifies the effective dielectric constant of the system. Hughes and White [5, 6] subsequently identified the physical origin of these modes by considering the dielectric relaxation time (which is essentially the Maxwell-Wagner effect) and the fact that the propagating wave can be approximated by a quasi-transverse electromagnetic wave.

More recently, there has been an increasing interest in the use of coplanar waveguide (CPW) transmission lines in microwave and millimeter wave integrated circuits. The field configuration in a coplanar waveguide transmission line can be considerably more complex than that in a microstrip; however, one would expect qualitatively similar slow-wave propagation on both microstrip and CPW lines. Accurate analysis of CPWs on lossy, layered substrates has been performed using full wave techniques which takes into account the electric field distributions in the substrate [7, 8, 9, 10, 11, 12, 13]. These models clearly predict the occurrence of slow-wave effects, and suggest a number of designs of possible use in phase shifter applications. Experimental verification of the existence of slow-wave propagation with coplanar waveguide structures has also been obtained by several investigators [14, 15].

One difficulty with the numerically intensive analyses discussed above is the extraction of simple physical insight into device operation. Using a quasi-TEM approximation, however, it is possible to construct a simple model of dielectric-supported transmission lines which illustrate the main effects caused by a lossy layer in the substrate [15, 16, 17, 18]. Although this model will not yield exact results, it does allow the development of physical insight, which can guide the choice of structure which should be analyzed with the more accurate full wave techniques. The next section discusses this approach, which indicates how slow-wave propagation can be controlled to allow construction of a variable phase shifter.

IV. Parallel Plate Model of Slow Wave Transmission Lines

Figure 1 illustrates a typical coplanar waveguide structure fabricated on a multilayer substrate. In order to understand how such a transmission line can be used as a phase shifter, it is easiest to first determine how its propagation velocity varies with frequency. There are two key characteristic frequencies for such a device. One is determined by the penetration of the magnetic field into the lossy layer, i.e. the "skin depth" frequency f_{sd} at which the skin depth in the lossy layer is no longer large compared to the thickness of the layer. Under these circumstances the lossy layer can be treated as a ground plane, and the propagation velocity of the transmission line is largely determined by the dielectric constant of the topmost lossless layer in the substrate. This limit is approximately given by

$$f_{sd} = \frac{1}{\pi\mu\sigma(b_{lossy})^2} \tag{1}$$

where σ is the conductivity, and b_{lossy} the thickness, of the lossy layer. For frequencies above f_{sd} the device operates in the skin effect mode of propagation.

The second frequency limit for these devices is set by the dielectric relaxation frequency f_{dr} of the lossy layer

$$f_{dr} = \frac{\sigma}{2\pi\varepsilon_r\varepsilon_o} \tag{2}$$

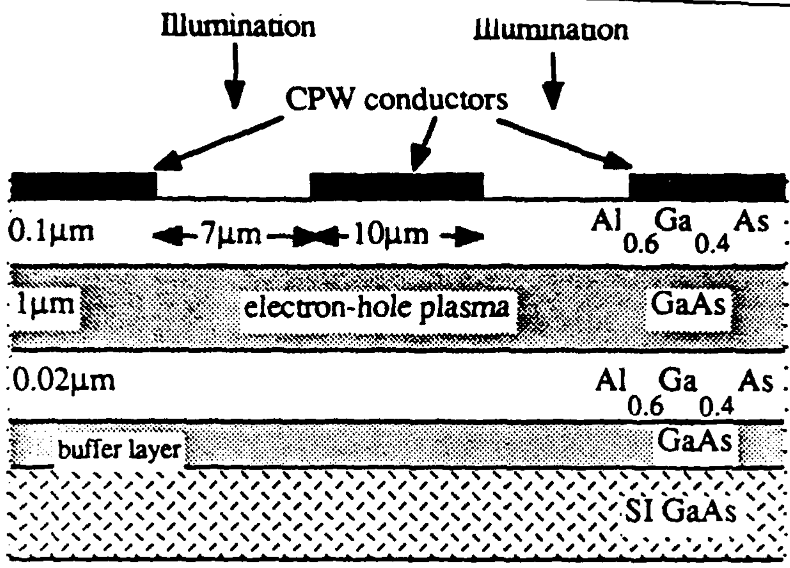

(a) Optically controlled coplanar waveguide phase shifter structure.

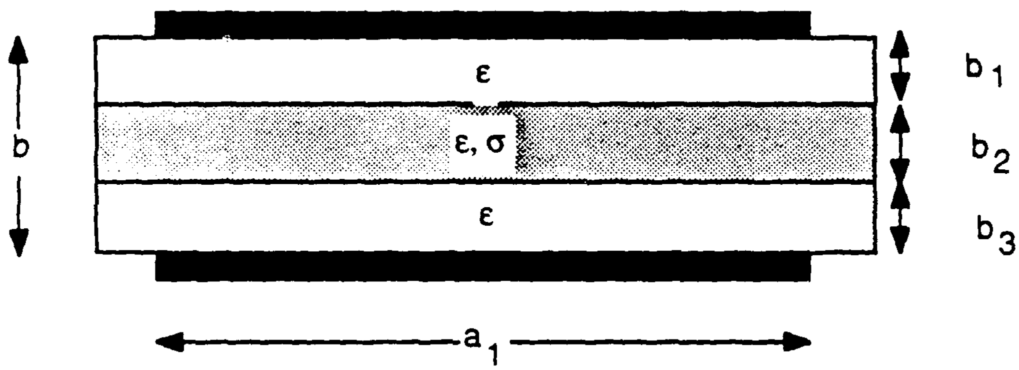

(b) Simple plane parallel plate waveguide model which exhibits slow wave behavior.

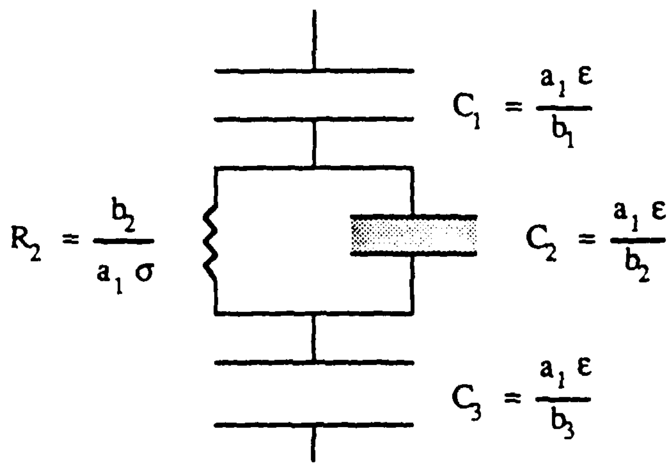

(c) Equivalent circuit for *shunt* admittance Y in transmission line model of the waveguide shown in (b).

Figure 1

where ε_r is the relative dielectric constant of the lossy layer. If the frequency of the applied signal is much greater than this frequency the free carriers in the lossy layer cannot respond to the signal; the lossy layer then appears as a simple dielectric between the top and bottom lossless layers in the substrate. For operation above f_{dr} this is referred to as the lossy dielectric mode of propagation.

If the relative dielectric constants of all the layers in the substrate are comparable, the phase velocity for either the lossy dielectric or the skin effect mode is approximately given by

$$v = \frac{c}{\sqrt{\varepsilon_{reff}}} \tag{3}$$

where c is the speed of light in vacuum. For a microstrip or CPW, ε_{reff} is the average dielectric constant of the substrate and air,

$$\varepsilon_{reff} = \frac{\varepsilon_r + 1}{2} \tag{4}$$

We now need to consider the behavior of the transmission line for frequencies much less than f_{dr} or f_{sd}. This can most easily be determined by using conventional transmission line analysis where the line is characterized by its equivalent series impedance per unit length Z_l and shunt admittance per unit length Y_l. The complex characteristic impedance of the line is then

$$Z_o = \sqrt{\frac{Z_l}{Y_l}} \tag{5}$$

and the complex propagation constant is

$$\gamma = \sqrt{Z_l Y_l} \tag{6}$$

It is illustrative to examine how these transmission line parameters would behave for a simple parallel plate waveguide. Figure 1 (b and c) illustrates the model used here. The parallel plate waveguide is filled with a layered dielectric between the plates of the guide. So long as the dielectric constants and conductivities of each layer are not too different, this guide will support a quasi-TEM mode of propagation. The slow wave structure shown in Fig. 1 contains three layers of dielectric. The top and bottom layers are lossless with relative permittivity ε_r, while the center layer is lossy with conductivity σ. In terms of the response of the structure to an applied voltage, if the frequency of the applied voltage is much less than the dielectric relaxation frequency f_{dr} in layer 2 given by eq. 2, then the free charges in layer 2 can respond to the applied voltage so rapidly that it essentially forms a short between the two cladding dielectric layers. Here $Y_l = j\omega C$, where the capacitance/unit length C of the structure is

$$C = \varepsilon\, a_1 \frac{1}{b_1 + b_3} = \varepsilon\, a_1 \frac{1}{b - b_2} \tag{7}$$

When the frequency is such that $f >> f_{dr}$ the free charges in layer 2 can no longer follow the applied field, and the capacitance is that of a parallel plate capacitor filled with a uniform dielectric material of permittivity $\varepsilon = \varepsilon_r\varepsilon_o$. The capacitance/unit length C is thus reduced, and is now

$$C = \varepsilon\, a_1 \frac{1}{b} \tag{8}$$

For a frequency low enough that the skin depth in the lossy layer is much greater than the thickness of this layer (i.e., $f << f_{sd}$), the inductance per unit length for the transmission line is approximately the quasi-static value of the entire structure. The inductance/unit length is then given by

$$L = \mu \frac{b}{a_1} \tag{9}$$

Using $Z_l = j\omega L$ and eq. 6, the propagation velocity v is given by

$$v = \frac{\omega}{\mathrm{Im}(\gamma)} = \frac{1}{\sqrt{LC}} \tag{10}$$

Thus, for low frequencies the phase velocity is

$$v = \frac{1}{\sqrt{\mu \varepsilon_r \varepsilon_o}} \sqrt{\frac{b - b_2}{b}} = \frac{c}{\sqrt{\varepsilon_r}} \sqrt{1 - \Delta} \tag{11}$$

where $\Delta = b_2/b$ is the fractional amount of the guide filled with lossy material, and c is the speed of light in a vacuum. For high frequencies, i.e. $f >> f_{dr}$, the phase velocity increases, and is just that foı ıhe lossy dielectric mode given by eq. 3.

The magnitude of this effect depends critically on the relative fraction of lossy to lossless dielectric in the substrate. This is most easily seen for a parallel-plate waveguide, where the lossy filling fraction, Δ, is exactly the ratio of the lossy layer thickness to the total separation between the plates (see Fig. 1b, where $\Delta = b_2/b$). In a coplanar waveguide or microstrip the filling fraction would be determined using a conformal mapping technique. Under the conditions described above, the phase velocity is approximately

$$v = \frac{c}{\sqrt{\varepsilon_{reff}}} \sqrt{1 - \Delta} \tag{12}$$

Thus, the low frequency phase velocity is decreased compared to the high frequency value (eq. 3) by a factor of $\sqrt{1 - \Delta}$; this is the slow wave mode of propagation. We can now clearly see the origin of the slow wave phenomenon: at low frequencies the effective capacitance of the structure is increased relative to that at high frequencies, thus leading to a slower propagation velocity.

Since the phase delay produced when a wave propagates through a transmission line is inversely proportional to the phase velocity, it is somewhat more convenient to define the effective index of refraction of the guide, n_{eff} (also referred to as the slow wave factor), using

$$n_{eff} = \frac{c}{v} \tag{13}$$

For most structures, the slow wave mode of propagation dominates the behavior of the transmission line if the operating frequency is less than the "s' ›w wave" frequency f_{SW}, given by

$$f_{SW} = f_{dr}(1 - \Delta) \tag{14}$$

The slow wave ($f < f_{SW}$) effective index for the transmission line, then, is increased over that at high frequency ($f > f_{dr}$ or f_{sd}) by a factor of $(1 - \Delta)^{-1/2}$.

These frequency limits produce characteristics of the type shown in Fig. 2. Given a fixed frequency, as the conductivity of the lossy layer is increased, the characteristic propagating mode changes from a lossy dielectric mode to a slow wave mode, due to the change in effective capacitance of the structure. As the conductivity is further increased, the slow wave mode eventually changes to a skin effect mode. In contrast, for fixed conductivity, as the frequency is increased, the slow wave mode (higher effective index n_{eff}) eventually changes to either a lossy dielectric mode or skin effect mode (both with lower n_{eff}), depending on whether $f_{dr} < f_{sd}$ or $f_{sd} < f_{dr}$, respectively.

As noted above, the phase delay experienced as a wave passes through a transmission line is proportional to the effective index n_{eff}. Since Fig. 2 indicates how n_{eff} varies with the lossy filling fraction Δ and the conductivity σ of the lossy layer, we can begin to see how these lines could be used as a phase shifter for a fixed frequency. If the thickness of the lossy layer (and hence Δ) could be controlled, eqs. 12 and 13 show how the effective index n_{eff} would vary, assuming $f < f_{SW}$. One way to achieve this control is through the use of Schottky contacted metal lines on a doped semiconductor (Fig. 3a) [5, 6, 9, 19, 20, 21]. Under reverse bias, the depletion layers formed below the metal contacts have no free carriers, and so form the top lossless layer in the substrate. When the bias is changed, the thickness of the depletion layer changes, causing a corresponding change in Δ. This produces a change in the dispersion curve for the transmission line, as shown in

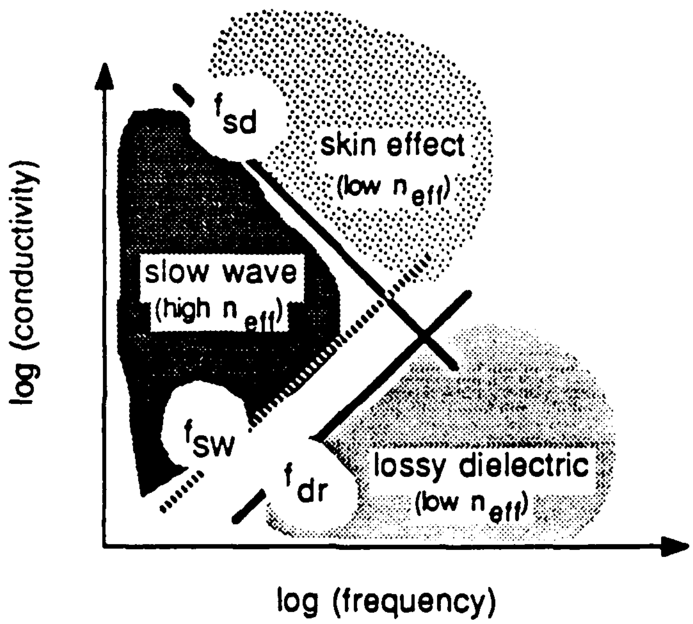

log (conductivity)
f_{sd}
skin effect
(low n_{eff})
slow wave
(high n_{eff})
f_{sw}
f_{dr}
lossy dielectric
(low n_{eff})
log (frequency)

Figure 2

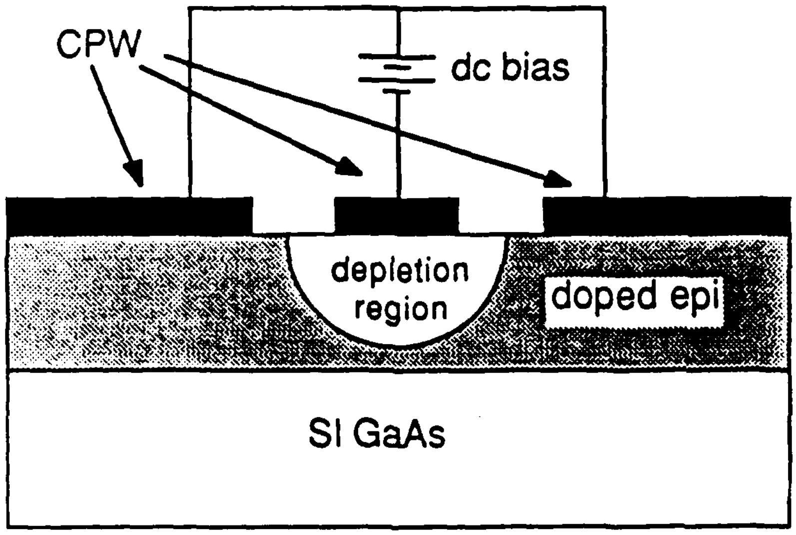
CPW
dc bias
depletion region
doped epi
SI GaAs

(A)

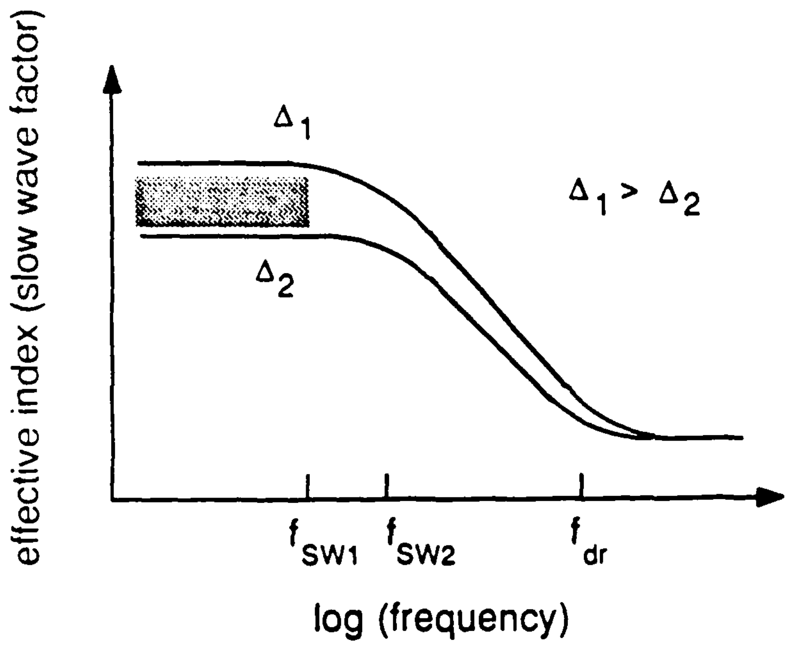
effective index (slow wave factor)
Δ_1
$\Delta_1 > \Delta_2$
Δ_2
f_{SW1} f_{SW2} f_{dr}
log (frequency)

(B)

Figure 3

Fig. 3b. A voltage controlled phase shift will then be produced if the frequency of operation is below the dielectric relaxation frequency f_{dr}. Maximum change in phase will be achieved only if the operating frequency is below f_{SW}, so that maximum change in n_{eff} is attained. Large values and large changes in n_{eff}, and hence large phase shift capability, are most easily obtained for values of Δ close to one, as shown by eqs. 12 and 13.

There is another possible way to control the propagation velocity on a slow wave transmission line, as illustrated by Fig. 4a. Here the conductivity of the lossy layer is varied directly; this change in conductivity moves the operating point of the device between the lossy dielectric region and the slow wave region. To obtain phase shift the frequency of operation should now be chosen in a regime of strong dispersion, roughly between f_{SW} and f_{dr}. The easiest way to externally control the conductivity of the lossy layer is via an optically induced electron-hole plasma in the semiconductor. This is the basis for the simplest optically controlled phase shifter [22] under study here.

The simple model discussed above can be used to estimate the behavior of these devices. Figure 5 illustrates the effect of varying the percentage Δ of the dielectric substrate which is lossy. Since all the frequency dependent behavior scales with the dielectric relaxation frequency, the frequency is given in units of $f_{dr} = \sigma/2\pi\varepsilon$. The units of n' and n'' are scaled to $\sqrt{\varepsilon_r}$. The slow wave factor n' clearly exhibits a strong dependence on the amount of lossy material, with a maximum normalized slow wave factor of 10 for 99% lossy dielectric. Examination of Fig. 5 shows that the frequency at which the slow wave factor begins to drop corresponds to f_{SW} (eq. 14). As the frequency is increased beyond f_{dr} (which equals one in normalized units), the propagating mode is no longer slow, but has changed to a lossy dielectric mode.

Figure 5 also clearly illustrates the difference between the two control methods, i.e. Schottky and optical. With Schottky control the variable Δ is directly controlled, so the effect is to shift from one curve to another in Fig. 5, while remaining at a fixed normalized operating frequency (since σ is fixed). Thus, for Schottky control it is desirable to

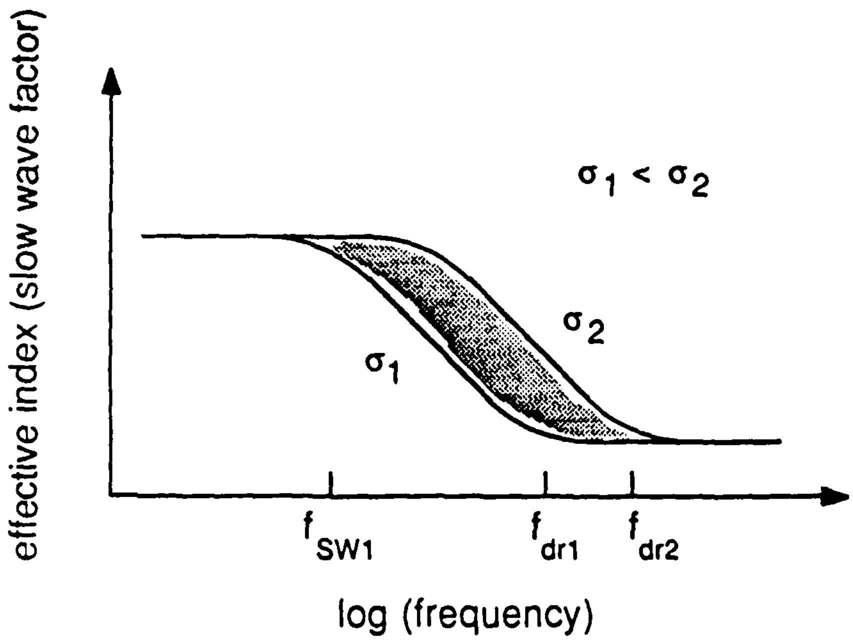

effective index (slow wave factor)
σ1 < σ2
σ2
σ1
fSW1
fdr1
fdr2
log (frequency)

(A)

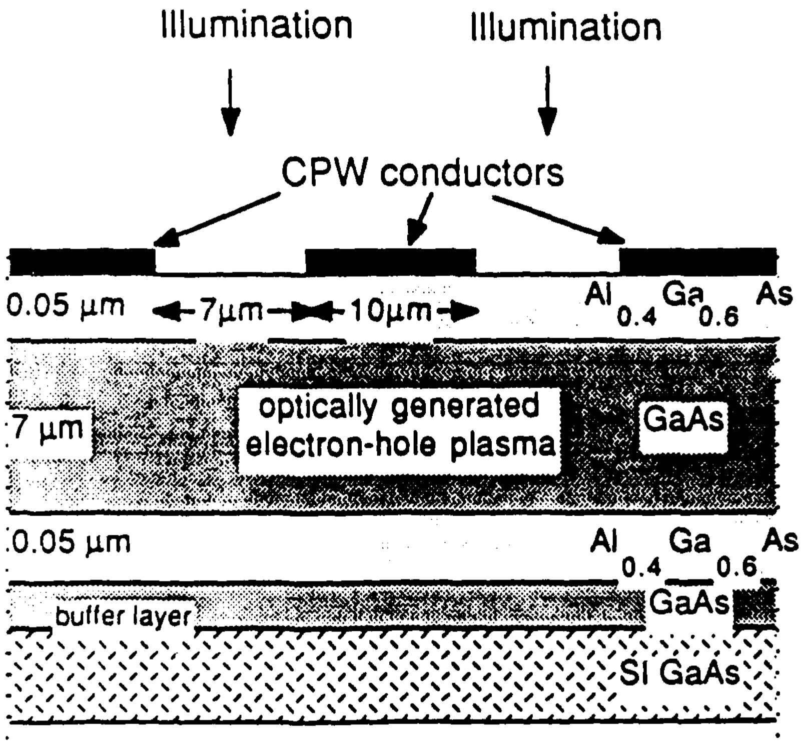

Illumination
Illumination
CPW conductors
0.05 μm
7μm
10μm
Al 0.4 Ga 0.6 As
7 μm
optically generated electron-hole plasma
GaAs
0.05 μm
Al 0.4 Ga 0.6 As
buffer layer
GaAs
SI GaAs

(B)

Figure 4

operating at "low" frequency, i.e. $f << f_{SW}$, in the flat part of the dispersion curve. Figure 6 illustrates how such a device might behave, assuming the material system is GaAs doped to 10^{17} cm^{-3}. In this case $f_{dr} \approx 10^{14}$ Hz, while f_{SW} varies from 10^{12} Hz for $\Delta = 99\%$ to 7×10^{13} Hz for $\Delta = 30\%$. Thus, this device could in principle be used beyond 100 GHz, and provide slow wave factors of up to about 35.

In contrast to the Schottky control technique, optical control varies the conductivity of the lossy layer rather than its thickness. In such a case, in Fig. 5 the device would always operate on curve of fixed Δ; slow wave control would be obtained through a variation in the normalized frequency of operation, f_{op}/f_{dr}, via a variation in σ. Here it is necessary to operate in a region of strong dispersion to achieve large phase shifts, as illustrated in Figs. 4 and 7. The requirements on operating frequency now become

$$f_{SW}(\sigma_{low}) < f_{op} < f_{SW}(\sigma_{high}) \tag{15}$$

where σ_{low} is the conductivity for low levels, and σ_{high} for high levels, of illumination intensity. To assure the frequency of operation is below f_{dr} σ must be fairly high, and hence the optically induced carrier densities must also be fairly large (for electrons at a carrier concentration of about 10^{15}cm^{-3} f_{dr} is about 100 GHz). Also note it is essential to use values of Δ which are large enough to simultaneously place f_{SW} below the frequency of operation. The example shown in Fig. 7 required $\delta = 99\%$ in order to allow large changes in slow wave factor near 100 GHz.

In addition to predicting the variation of propagation velocity, this model can also be used to estimate changes in the characteristic impedance of the transmission line. Equation 5 leads to

$$Z_o(f, \delta) = \frac{Z_o}{n'(f, \delta)} \tag{16}$$

where Z_o is the characteristic impedance of the structure at high frequencies, and $n'(f,\delta)$ is found from eqs. 12 and 13. Thus, the impedance of the guide should be inversely

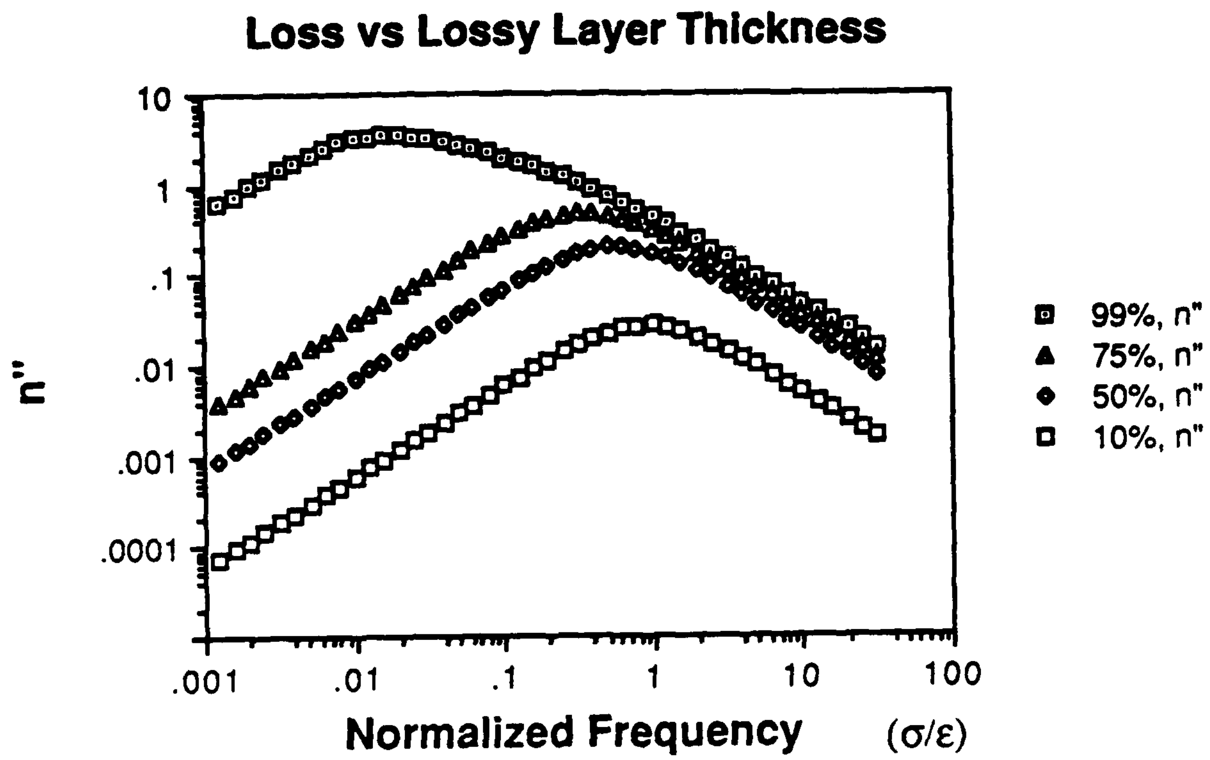
Loss vs Lossy Layer Thickness
n''
10
1
.1
.01
.001
.0001
.001
.01
.1
1
10
100
Normalized Frequency (σ/ε)
99%, n"
75%, n"
50%, n"
10%, n"

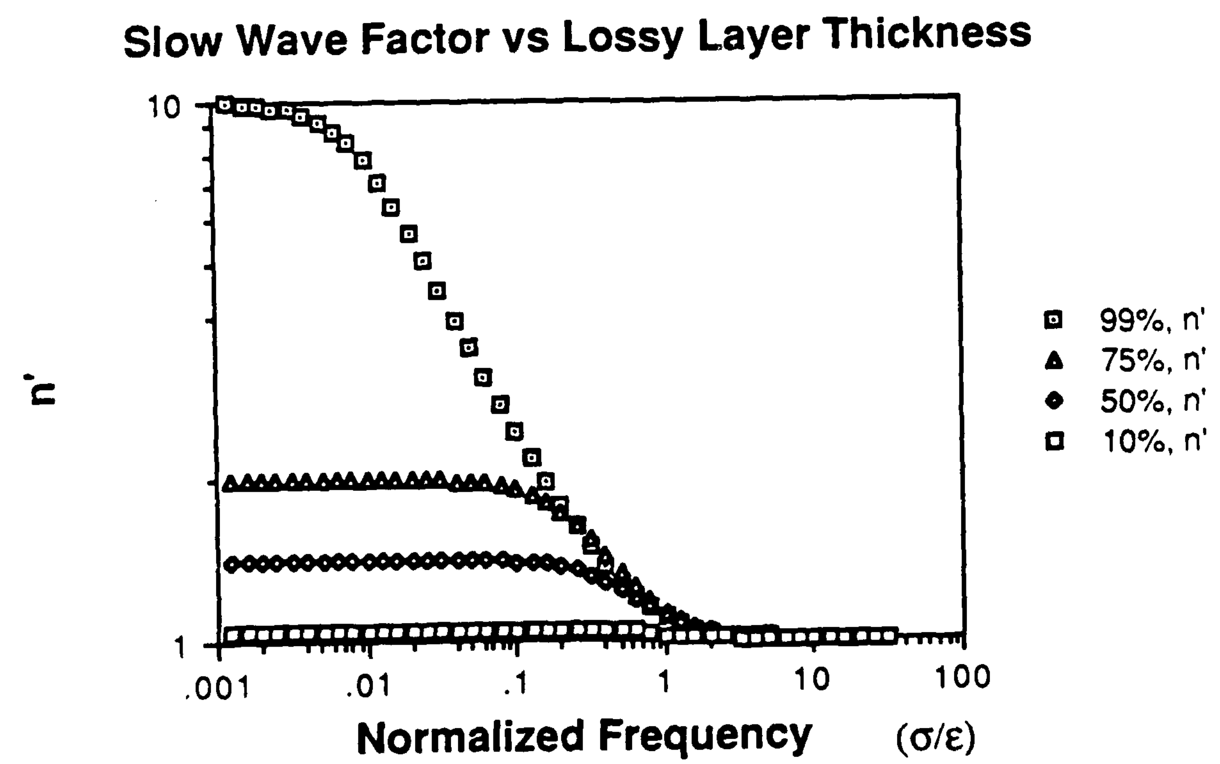
Slow Wave Factor vs Lossy Layer Thickness
n'
10
1
.001
.01
.1
1
10
100
Normalized Frequency (σ/ε)
99%, n'
75%, n'
50%, n'
10%, n'

Figure 5

Loss vs Lossy Layer Thickness

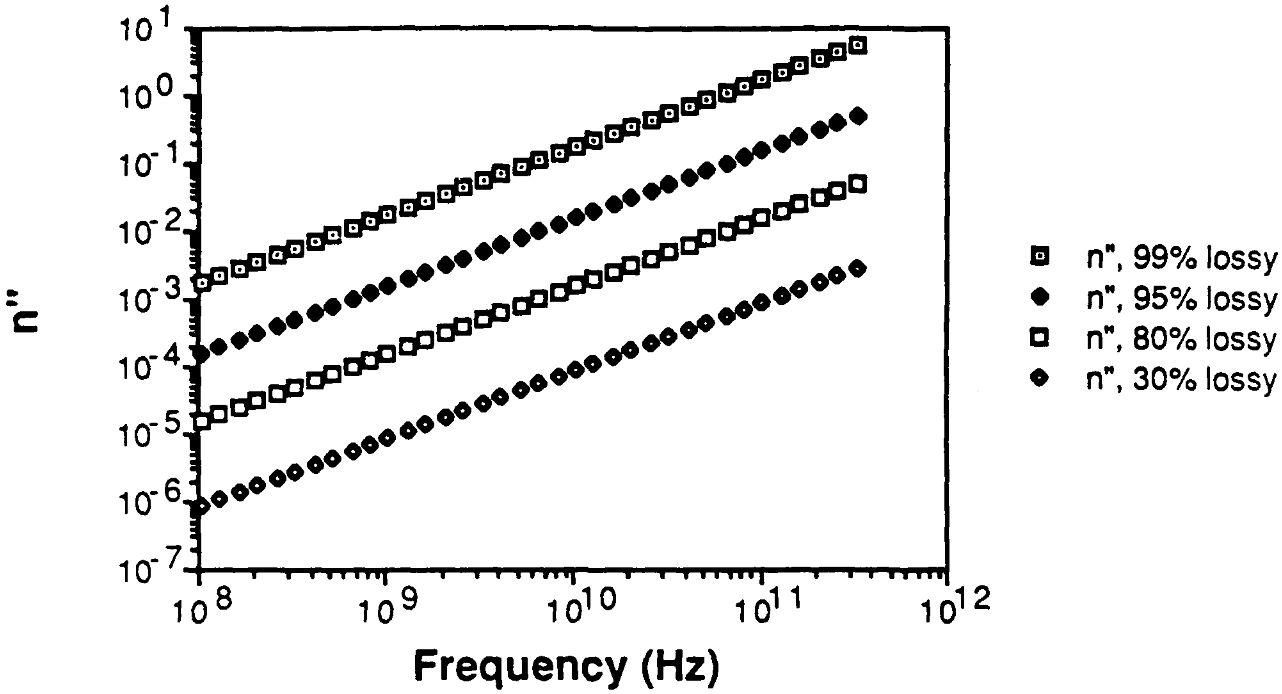

Slow Wave Factor vs Lossy Layer Thickness

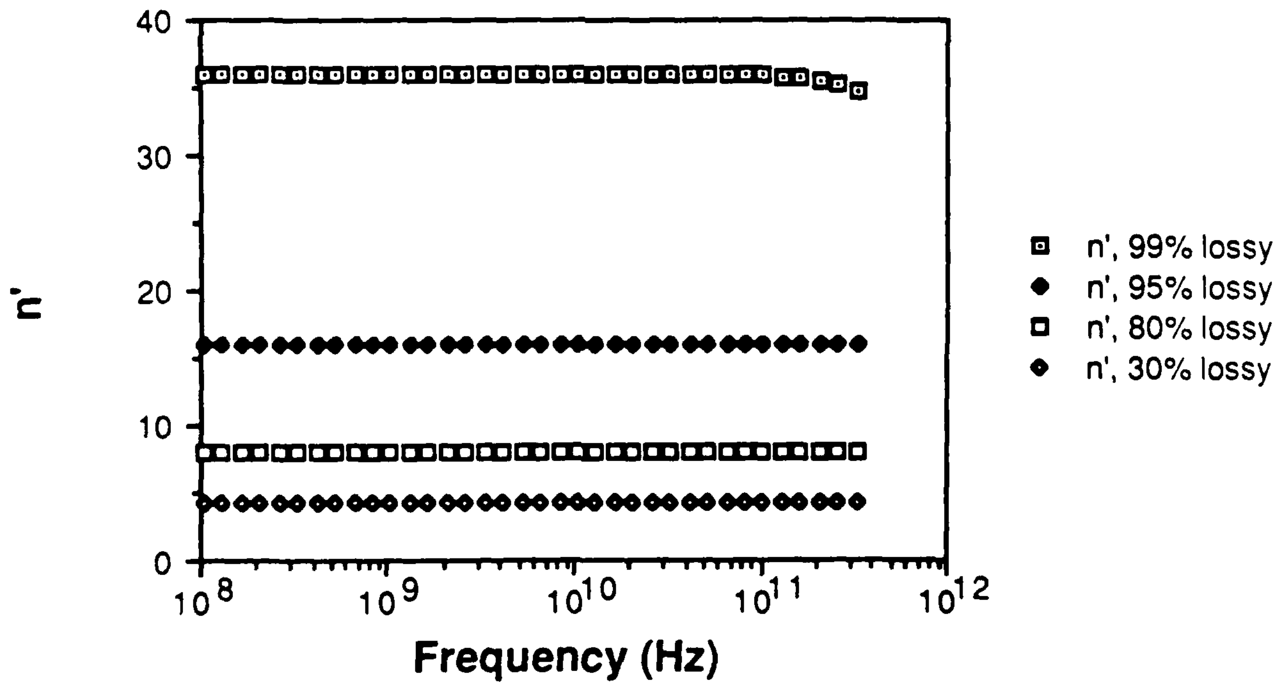

Figure 6

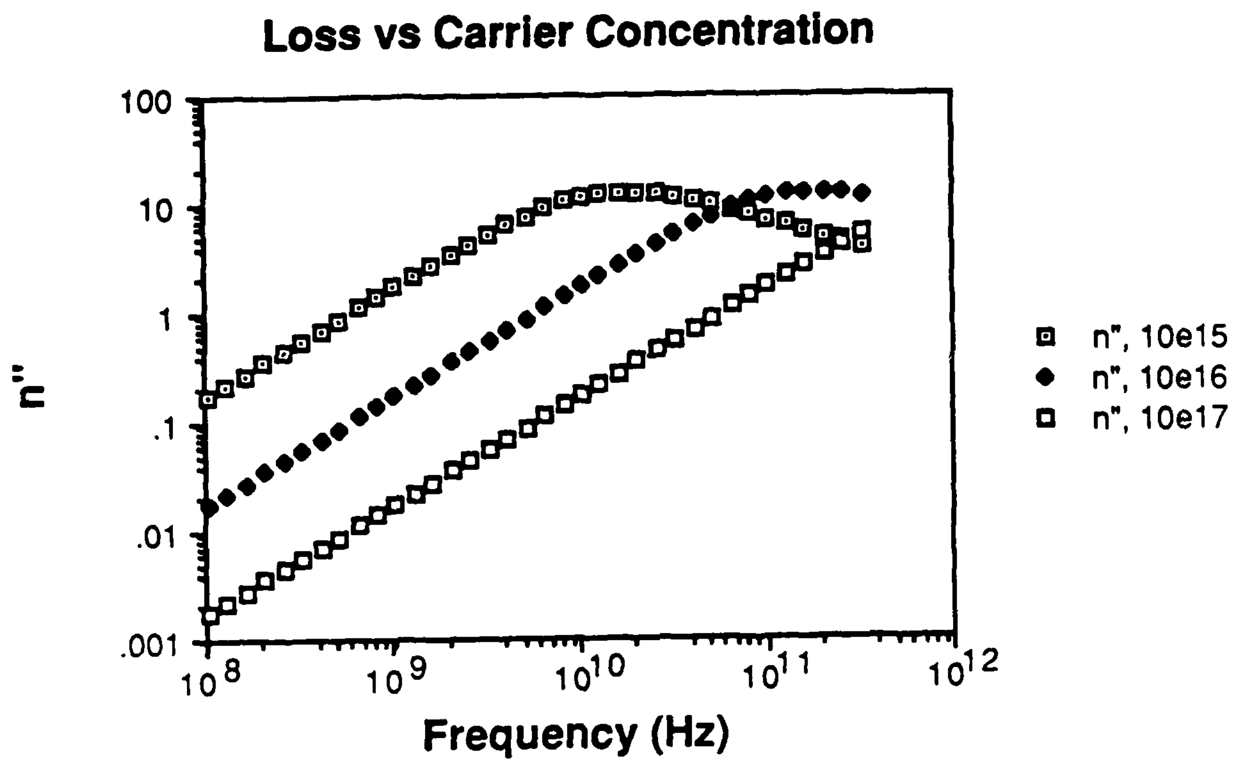

Loss vs Carrier Concentration
100
10
1
.1
.01
.001
n"
10^8
10^9
10^{10}
10^{11}
10^{12}
Frequency (Hz)
n", 10e15
n", 10e16
n", 10e17

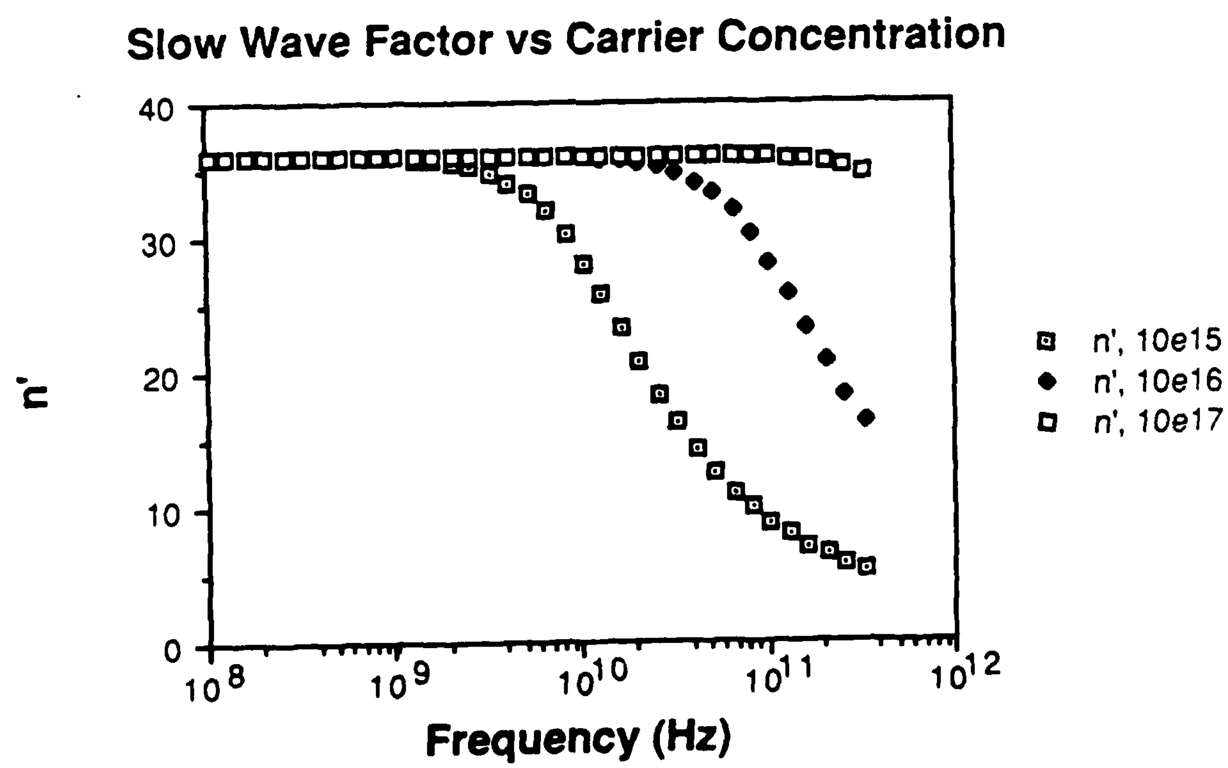

Slow Wave Factor vs Carrier Concentration
40
30
20
10
0
n'
10^8
10^9
10^{10}
10^{11}
10^{12}
Frequency (Hz)
n', 10e15
n', 10e16
n', 10e17

Figure 7

proportional to the slow wave factor. This may be an important factor in determining the return loss for these phase shifters.

V. Schottky-Contacted Slow Wave Phase Shifters

As discussed above, a variable phase shifter may be implemented electronically using Schottky-contacted microstrip or CPW conductors [23, 24, 25, 26, 27, 28]. A reverse bias is used to vary the depletion layer thickness [Fig. 3a], and hence the phase delay experienced, as the wave propagates through a fixed length of line. For a CPW, if only the central conductor is reverse biased, the depletion layer will be localized under this conductor. Ideally the depletion layer forming the first insulating layer should extend uniformly across from ground plane to ground plane. However, since a significant fraction of the field lines pass directly underneath the central conductor, the depletion region under the central conductor can still be used to control the slow-wave factor.

A number of Schottky-contacted phase shifters have been demonstrated to date. All of these devices have been rather short, ranging from 1.6 mm [20, 24, 25, 26] to 2.4 mm [27]. Such short lengths are possible because these devices make use of heavily doped layers (on the order of 10^{18} cm^{-3}), which produce large swings in the slow-wave factor, and consequently large changes in phase (for example, at 18 GHz, about 150^o / mm from [25], and 120^o / mm from [27]). The short length is useful, since it is then possible to save space on the semiconductor substrate. However, because Schottky contacts on highly doped substrates are difficult to fabricate, somewhat more complex processing steps are required. Often this is done by using a thin, lightly doped layer on top of the highly doped substrate. Most devices fabricated with these highly doped layers have also exhibited extremely high insertion loss per unit length (typically 5 - 10 dB / mm [25, 27]), although because of the very large phase shifts per unit length, acceptable performance can still be achieved.

VI. Optically-Controlled Phase Shifters

The technique of using optical illumination to obtain phase shift was first demonstrated using high resistivity semiconductor dielectric waveguides by Lee et al. [29, 30]. In their work, an optical source with wavelength shorter than the bandgap of the semiconductor generates a plasma layer near the surface of a dielectric waveguide, causing a change in the propagation constant for the guide, which in turn produces a phase shift. Assuming a uniform electron-hole plasma is formed by the optical irradiation, extremely large phase shifts have been predicted [30] for very high plasma densities. A very intense source of illumination is used to produce the large carrier concentrations. Typically, a powerful pulsed laser has been used. An additional feature of this kind of phase shifter is its potentially high speed. By using Cr-doped GaAs with very short carrier lifetimes in conjunction with picosecond optical pulses, Li et al. [31] demonstrated modulation of a 94 GHz signal with switching times on the order of 100 ps.

A similar approach for controlling the propagation constant in a CPW could also be used. The conductivity of the lossy layer, which depends on the density of the electron-hole pairs generated, is controlled by varying the intensity of the optical illumination. As in the dielectric waveguides, depending on the carrier lifetimes in the semiconductor, the speed of such a device could be very high. However, as discused in Section IV, for this technique to be effective the conductivity of a large fraction of the substrate must be controlled, and therefore accessible to the effects of the optical illumination. In this regard, a CPW transmission line is much better suited for optical control than is a microstrip line. This is because virtually all field lines extend across the gaps between ground plane and central conductor, which is also where the electron-hole pairs are generated. For a microstrip, the central conductor casts a shadow in the region where most field lines are concentrated. In addition, for a CPW the optically-generated carriers may diffuse into the region shadowed by the central conductor, so long as the width of the central conductor does not exceed the diffusion length in the semiconductor. To satisfy this condition in a microstrip line would require the use of extremely thin substrates.

Another issue which should be considered for both optically controlled dielectric waveguides and CPWs is the impact of spatially nonuniform carrier generation. For both devices a combination of surface recombination and diffusion will produce nonuniform carrier distributions. In an analysis by Butler et al. [32] it was shown that phase shift is not dramatically effected in a dielectric waveguide, although there may be a considerable increase in attenuation. For a CPW, analysis using finite element methods shows that a uniform carrier density needs to be maintained a distance under the ground planes equal to the gap width for the propagation characteristics to be unaffected [33]. A quasi-static analysis including the effects of carrier diffusion has also been developed [34]. This model yields insertion loss estimates for CPWs with optically induced electron-hole plasmas.

The optically controlled CPW device shown in Fig. 4b makes use of a heterojunction substrate which is chosen to allow optical carrier generation to take place in a buried layer instead of at the surface. For the material system AlGaAs/GaAs/AlGaAs, a light source with energy below the band gap for the AlGaAs layer but well above that of the GaAs layer can be selected. When the substrate is illuminated by this source, electron-hole pairs are generated only in the GaAs layer. The band gap discontinuity between the AlGaAs/GaAs layer presents a barrier to the diffusion of the electron-hole plasma out of the GaAs layer, thus confining the optically-generated carriers. The AlGaAs layer also serves to passivate the GaAs, producing a reduced surface recombination velocity ($\approx$ 400-500 cm/sec for a AlGaAs/GaAs interface compared to 10^6-10^7 cm/sec for an GaAs/air interface); this allows more efficient generation of carriers by the optical illumination [35]. A layered-substrate approach has also been discussed for use in dielectric waveguide phase shifters. The analysis by Scott et al. [36] showed lower attenuation for this approach, while maintaining similar phase shifts.

A major constraint on the operation of the devices discussed above is the requirement that the optically-generated carriers significantly effect the conductivity of the layer. This requires raising the optically-generated carrier concentration to near or above that of the background doping. In previous work excess carrier densities were assumed or calculated using low-level injection approximations (even though high power pulsed lasers were used to provide sufficient carrier generation), and a Drude-Lorentz model used to determine the complex dielectric constant of the plasma layer. Since wave propagation is only modified by excess carrier densities greater than the background doping level, to determine optically-generated carrier concentrations it is important to solve the diffusion equation in a high-level injection regime. We have solved the general nonlinear diffusion equation, including the dependence of the ambipolar diffusion constant and recombination rate on carrier density n(x):

$$-\left[\frac{D_n\,(2 + N_A/n)}{1 + \mu_n/\mu_p + N_A/n}\right]\frac{d^2n}{dx^2} + (1/\tau + Bn)\,n = I_o\,\delta(x)$$

where D_n is the minority carrier diffusion coefficient, N_A is the background doping level (p-type assumed here), μ_n and μ_p are respectively the electron and hole mobilities, τ is the minority carrier lifetime for low level injection, B is the direct electron-hole recombination coefficient, and I_o is the illumination intensity in photons/cm^2. In our calculations we assume $N_A = 10^{15}\text{cm}^{-3}$, and for GaAs at room temperature: $D_n = 180\text{cm}^2/\text{sec}$, $\mu_n/\mu_p = 20$, $\tau = 800\text{nsec}$, and $B = 2\times10^{-10}\text{cm}^3/\text{sec}$. The optical generation term is approximated by a delta function at the front surface since the absorption coefficient well above the band gap is much larger than any diffusion lengths in the solution. The differential equation is solved numerically for a 0.5mm thick layer, subject to a front boundary condition which includes surface recombination, and a back boundary condition that simulates the effect of an infinitely thick layer. Although the GaAs layer in our device is only microns thick, we calculate carrier densities for a very thick layer to allow for the effects of lateral diffusion away from the illuminated zones. We also restrict our calculations to carrier densities below $5x10^{17}cm^{-3}$, the point at which the quasi-fermi level for the electrons enters the conduction band. Figure 8a shows a plot of surface excess carrier density as a function of illumination intensity, and Figure 8b shows two carrier profiles for low and high level illumination. The carrier profiles decrease by no more than a factor of two in 10μm for high intensity cases, and are fairly constant over 10μm for lower levels of excitation. However, this shows that for a CPW device fabricated on a AlGaAs/GaAs substrate continuous wave (CW) illumination intensities in the Watts/cm^2 range are probably required to produce significant phase shift [22].

VII. Theoretical Studies Carried Out Under This Grant

ii) Simulation of CPW Propagation on Non-Uniform Substrates

A method based on the finite element algorithm has been developed for the analysis of the effect of laterally localized lossy regions on slow wave propagation in coplanar waveguides [33]. Since in a real optically-controlled CPW we would illuminate through the gaps between the CPW conductors, it might be expected that the mode matching model (which assumed laterally uniform layers) used in the earlier portions of our study might predict performance significantly different from actual devices. This new model allows the dielectric constant and conductivity of the substrate to vary in directions both perpendicular and parallel to the plane of the guide. The method is based on the finite element method but it is extended here to handle a problem involving complex arithmetic. This modification is necessitated by the fact that the structure is essentially lossy and hence the propagation constant is a complex number. Because of this modification, the algorithm developed could not be considered stationary. In the present case, the accuracy of the method has been established by numerically testing for a lossless case.

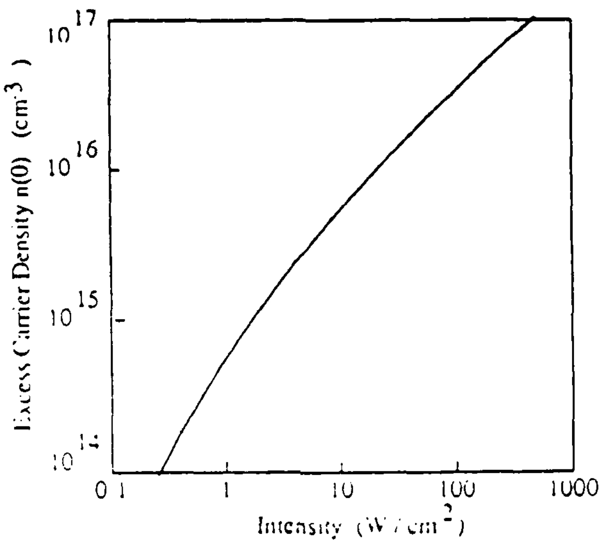

Optically generated carrier densities in the GaAs layer at the illuminated interface.

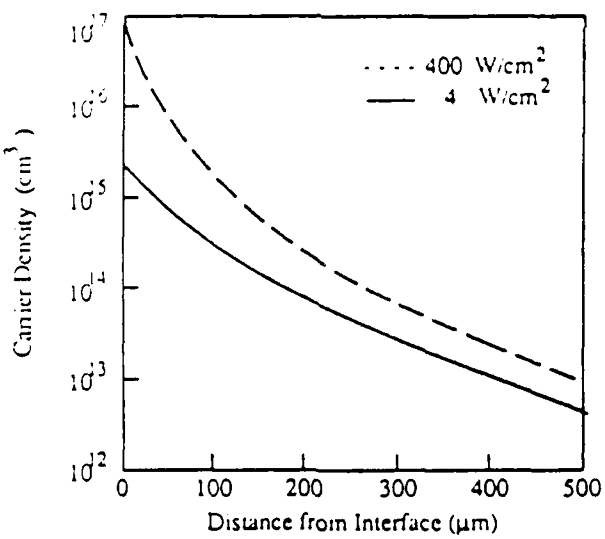

Carrier profiles predicted by nonlinear diffusion equation for two different intensities.

Figure 8

Once the method was developed, the algorithm was applied to a number of cases. In the earlier trials, we have applied the algorithm for a phase shifter structure in which the doped layer has a uniform conductivity in the lossy layer, generated by optical illumination. The method has now been applied to a structure with a non-uniform lossy GaAs layer. It was assumed diffusion yields a uniform carrier concentration under the narrow central conductor, but that the concentration fell off by an order of magnitude about 12μm from the illuminated edge under the ground planes. The finite element numerical results showed that such non-uniformity has little effect on the device performance in a steady state condition. However, time domain results show it may play an important role in analyzing transient phenomenon.

ii) Periodically Illuminated CPW

In the hope of reducing loss, a structure illuminated periodically along the wave propagation direction has also been analyzed [37]. Here, the structure is made of a successive chain of alternating lossy and lossless coplanar waveguides (see Figure 9). The primary objective is to find out if it is possible to create a structure which has a reduced insertion loss and yet retain a slow wave factor of about the same value as the uniformly illuminated structure. If the length of the period is much smaller than the wavelength, the only effect we obtain is a reduced slow wave factor accompanied by a reduced insertion loss. These reductions are in proportion to the duty factor within the period. One important case is one in which the length of the period is approximately one half of the wavelength; for this case a Bragg reflection occurs in a lossless periodic structure, which can produce very large phase shifts slightly off resonance.

To analyze this structure we first use the spectral domain technique to find the propagation constants and characteristic impedances of individual sections of lossless and lossy CPW transmission lines. The periodic structure is then modeled as a series of these

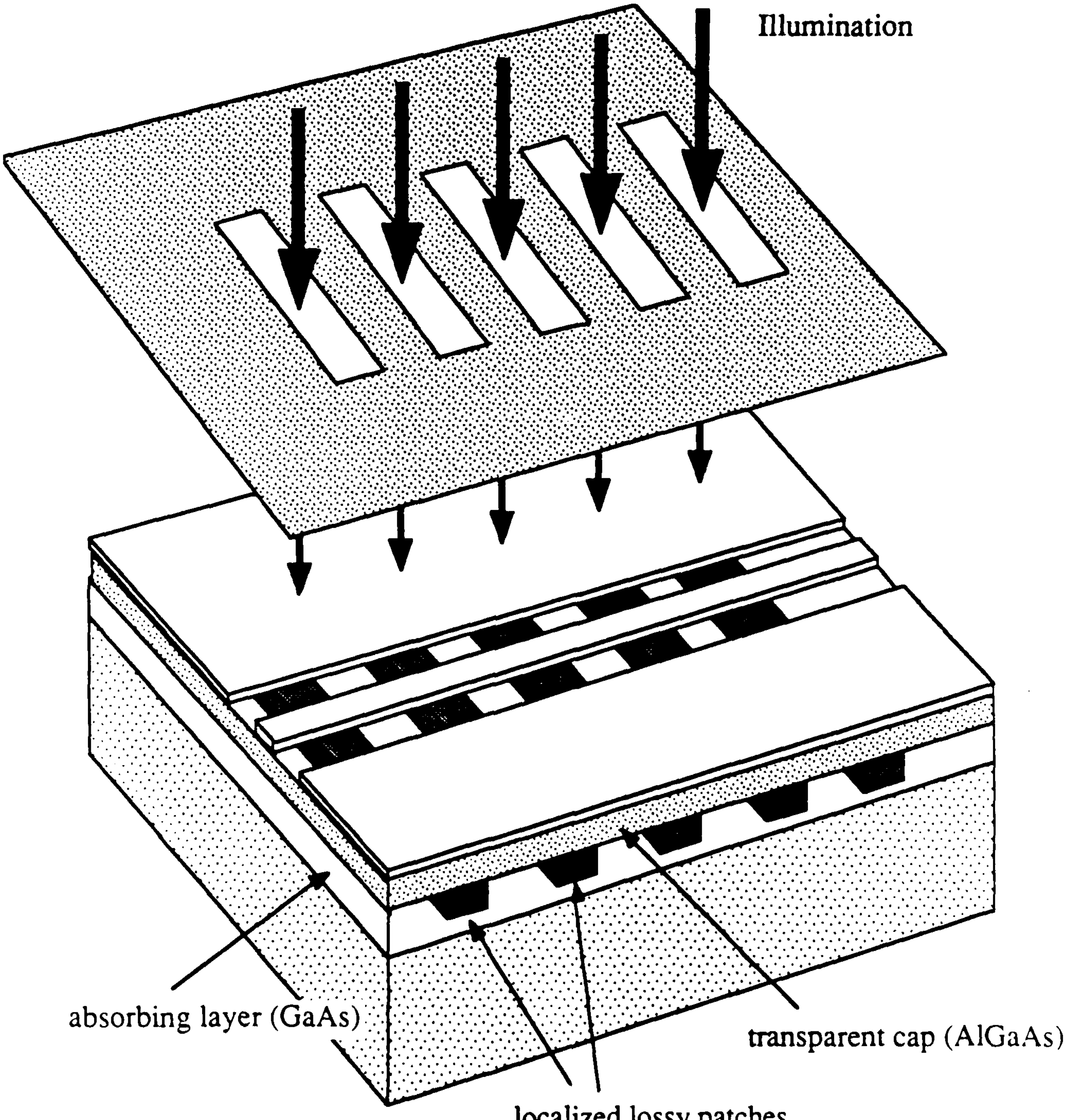
Illumination
absorbing layer (GaAs)
transparent cap (AlGaAs)
localized lossy patches

Figure 9

transmission lines, and the cascaded transmission line matrix calculated based on the spectral domain results. We have found that if the length of the period is much smaller than the wavelength, the only effect obtained is a reduced slow wave factor accompanied by a reduced attenuation loss. These reductions are in proportion to the duty factor (i.e. the ratio of lossless to lossy line). If a fixed phase shifting capability is required, these reductions exactly cancel one another, since a reduction in slow wave factor requires a longer line, which increases the final insertion loss.

When the period of the lossy/lossless sections becomes comparable to a guide wavelength resonant effects can occur. For instance, in a cascaded lossless line where only the characteristic impedances are varied Bragg reflection occurs if the length of the period is approximately one half of the wavelength. Near this point, strong dispersion can cause large phase shifts. This phenomenon does not occur in exactly the same way in our structures because the lines are lossy, although the calculations do indicate pass-band like characteristics.

We also used the calculations to locate an optimum set of parameters for a given design frequency. The initial calculations are for a structure with fixed total length and internal period, which makes it difficult to extract phase shifter design information. One advantage of the optical control technique is that one can easily vary the period, duty cycle, and carrier densities in the CPW lines to experimentally investigate this device.

VIII. Fabrication and Testing of Prototype CPW Phase Shifters

i) Optically Controlled Devices

To test the optically controlled CPW phase shifter, we have fabricated and tested several prototype devices on heterojunction substrates. The devices were fabricated using a lift-off technique based on a chlorobenzene soak process. A metal scheme of chrome/silver/gold with a total thickness of ~1.2 μm was used for the metal conductors.

Measurements on the devices were done with an HP 4194 Gain Phase Analyzer and an HP8510B automatic network analyzer in conjunction with wafer probes made by Design Technique. The epitaxial layer thicknesses and the device dimensions are given in Fig. 4b, except here the AlGaAs layers were 0.5 μm thick. The dimensions for the CPW were calculated using quasi-static methods to yield a 50 ohm characteristic impedance. For the AlGaAs mole fraction used (40% Al) all the conduction band valleys (Γ, L and X) of the AlGaAs layer are at about the same energy level above the conduction band (Γ valley) of the GaAs layer. In principle, by illuminating at a wavelength close to the band-gap of the GaAs layer, all the optically generated carriers should be well confined to the GaAs by the potential barrier due to the AlGaAs/GaAs band-gap discontinuities. The illuminating source used was a 1.0 Watt CW (total output power) GaAs laser diode array (SDL 2462P1) manufactured by Spectra Diode. The wavelength of the diode was 798 nm.

The results of the measurements are shown in Figs. 10 and 11. Figure 10 shows the phase shift of the device under the maximum level of optical illumination obtained with the laser diode. The optical intensity was approximately 3.5 Watts/cm^2. Figure 11 shows the accompanying insertion loss of the device. The insertion loss for the unilluminated case is relatively low, and only slightly greater than that for a semi-insulating substrate. This is due to both the thin, low conductivity AlGaAs layer, and the very light doping in the GaAs layer ($<10^{15}$cm^{-3}, p-type). Figure 12 shows the insertion loss with light on that would be encountered if this device where made long enough to provide 180^o of phase shift between the illuminated and unilluminated state. Since the phase shift obtained is relatively small such a phase shifter would have to be very long, generating very large insertion loss. The small phase shift is not surprising, since for the illumination intensities used the optically-generated carrier density is probably still less than the background doping concentration. In order to obtain larger phase shifts, sources with significantly higher optical intensity than that obtained with the laser diode must be used. This is a major limitation on the optical

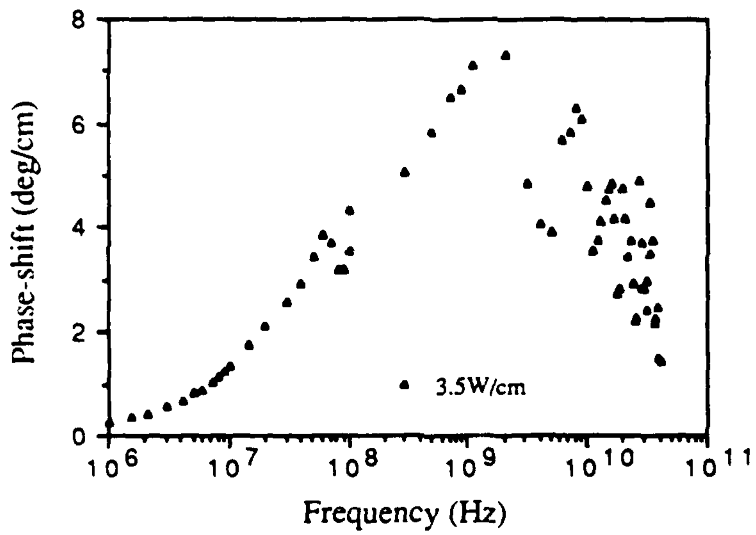
8
6
4
2
0
Phase-shift (deg/cm)
3.5W/cm
10^6
10^7
10^8
10^9
10^{10}
10^{11}
Frequency (Hz)

Figure 10

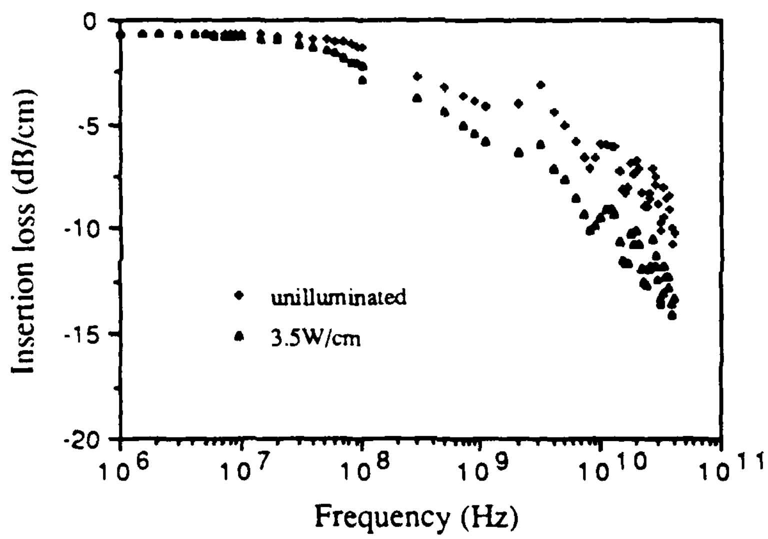
0
-5
-10
-15
-20
Insertion loss (dB/cm)
unilluminated
3.5W/cm
10^6
10^7
10^8
10^9
10^{10}
10^{11}
Frequency (Hz)

Figure 11

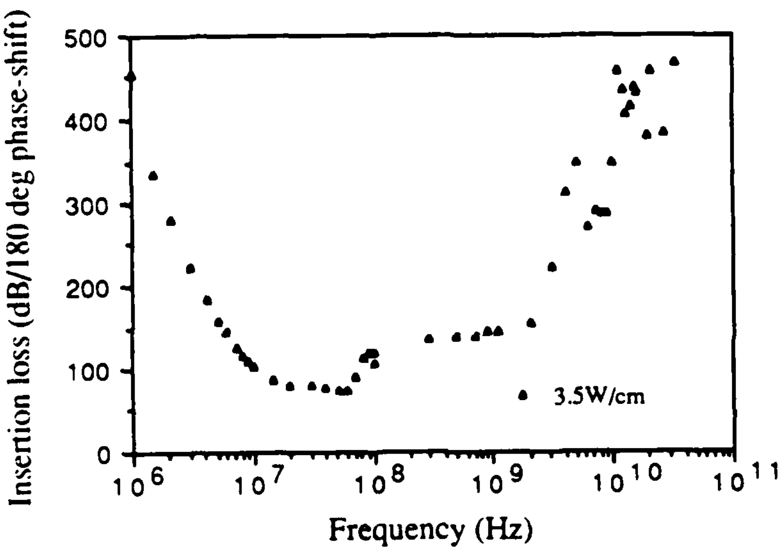
Insertion loss (dB/180 deg phase-shift)
500
400
300
200
100
0
3.5W/cm
10^6
10^7
10^8
10^9
10^{10}
10^{11}
Frequency (Hz)

Figure 12

control technique, since it would generally require large power supplies for the high intensity illuminator.

ii) Schottky-biased Optically Controlled CPW Phase Shifters

The preceding discussions clearly indicate that purely optically controlled phase shifters require the use of very high intensity optical sources. It would be desirable to reduce the illumination intensities required. One device which is very sensitive to low levels of illumination is a reverse-biased junction. For instance, the capacitance of such a junction can be changed quite easily, since carrier generation takes place within the depletion region, where background carrier concentration is extremely small. Herczfeld et al. first used this approach to build a hybrid phase shifter using discrete PIN diodes mounted across a CPW transmission line [38]. They used a fiber optic cable to illuminate the D.C.-biased PIN diodes, producing a phase shift of 10^{o}. To further improve the performance of the phase shifter, lateral PIN diodes have also been monolithically integrated into a CPW structure [39, 40]. Initial results for a reflection-type phase shifter gave total phase shifts of $110\text{-}120^{o}$ for frequencies between 1 and 3.5 GHz, and $150\text{-}170^{o}$ between 4 and 8 GHz.

The PIN diodes used above present a "lumped" circuit loading of the CPW. A logical extension of this approach is the use of a D.C. biased "distributed" Schottky diode to construct the entire CPW transmission line, in conjunction with optical illumination to control the propagation constant of the line (Fig. 13) [41]. With this device, we can control the thickness of the depletion layer, as in the Schottky-contact controlled method, but rather than varying the D.C. bias, we vary the optical illumination intensity. This should provide much greater optical sensitivity than the purely optically controlled approach, which required high level illumination to achieve appreciable phase shifts.

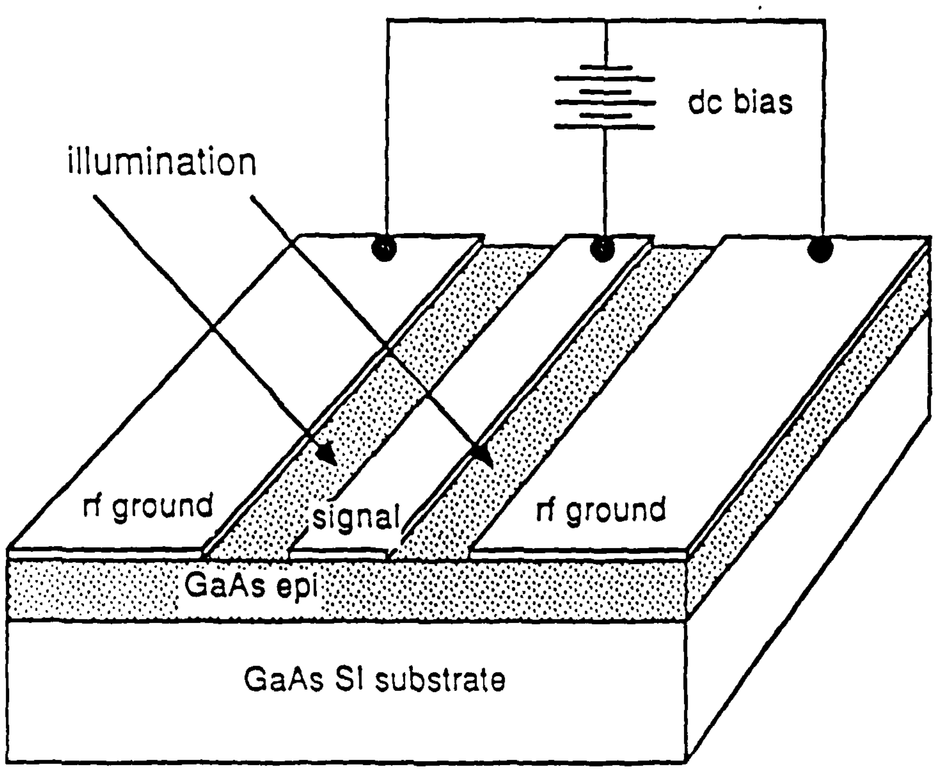
dc bias
illumination
rf ground
signal
rf ground
GaAs epi
GaAs SI substrate

Figure 13

To perform initial tests on a Schottky-contact/optically control CPW phase shifter, we have used an MBE-grown epitaxial GaAs layer on an SI GaAs substrate. The epitaxial layer used was 7 μm thick, with a p-type doping concentration in the low 10^{15} cm^{-3}. CPW devices were then fabricated on the substrate. The central conductor was held at a reverse bias of 35 volts dc, and the device was then illuminated with a filtered incandescent microscope illuminator. The filter cut off all wavelengths shorter than 740 nm, with spectral irradiance at longer wavelengths typical of a blackbody source. The phase shift and insertion loss of the device was then measured in the dark and under illumination. We used the two illuminating intensities of 2 and 4 mW/cm^2, integrated over the full bandwidth of the filtered source. Since light can be absorbed only through the gaps between the center conductor and the ground planes of the CPW, the device has an absorbing area of approximately 1.4×10^{-3} cm^2. Thus, the maximum absorbed optical power for the two intensities is about 3 and 6 μW, respectively. This represents an upper bound on the actual absorbed power, since any power at wavelengths longer than 867 nm is not absorbed by the GaAs.

The measured phase shift and insertion loss for this device as a function of illumination intensity is given in Fig. 14 (a) and (b). Note that this device exhibits extraordinary sensitivity to illumination. At 20 GHz, with 4 mW/cm^2 illumination (less than 6 μW absorbed power), the device showed a phase shift of 90°/cm (referenced to the unilluminated case) with 12 dB/cm of insertion loss. The largest phase shift measured here was about 120°/cm at 40 GHz for 4 mW/cm^2 illuminating intensity. Even at these very low intensities, evidence of optical saturation is seen, since doubling of the intensity produces significantly less than a doubling of the phase shift.

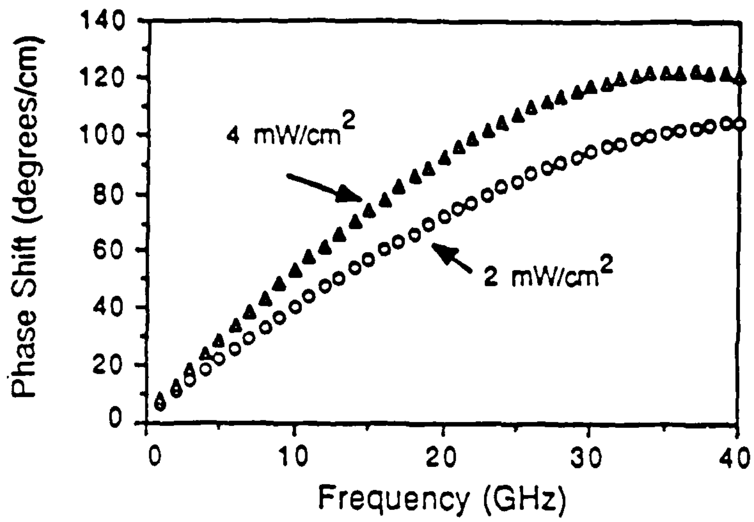

140
120
100
80
60
40
20
0
Phase Shift (degrees/cm)
4 mW/cm2
2 mW/cm2
0
10
20
30
40
Frequency (GHz)

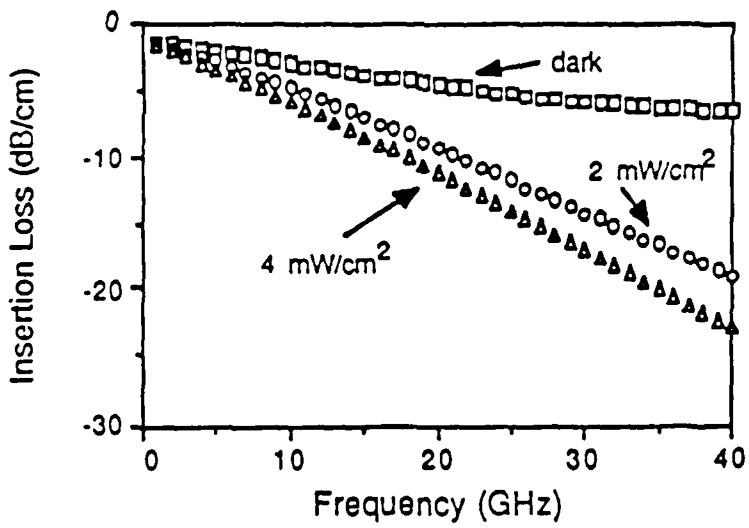

0
-10
-20
-30
Insertion Loss (dB/cm)
dark
2 mW/cm2
4 mW/cm2
0
10
20
30
40
Frequency (GHz)

Figure 14

The slow-wave factor (or the effective index of refraction n_{eff}) was calculated from the measured data using

$$SWF = \frac{\lambda_0}{\lambda_g} = n_{eff} = \frac{\theta c}{2 \pi \ell f} \tag{10}$$

where θ is the measured phase, ℓ is the physical length of the device, c is the speed of light and f is the frequency. Figure 15 shows n_{eff} for the Schottky-contacted/optically controlled device. The slow-wave factor of the device under bias but unilluminated is about 2.5. This is quite close to the quasi-static value of 2.67. It is also quite constant throughout the range of frequency measured, showing that the device is essentially dispersionless. As the illumination is increased n_{eff} increases to about 2.7, and begins to saturate as the optical intensity is increased further. The slow-wave factor, however, remains essentially dispersionless under optical illumination, as expected for a device in which control is via a change in the effective lossy layer thickness (Section IV and Fig. 4a).

An important measure of the performance of any phase shifter is the amount of insertion loss the device produces per degree of phase shift achieved. For all the devices based on slow-wave effects, this insertion loss also tends to vary as the phase is changed. Figure 16 shows the insertion loss of the Schottky-contact/optically controlled device per 180° of phase shift for 4 mW/cm^2 illumination. The insertion loss with no illumination is also shown in Fig.16; in operation, the loss would vary between this value and the 4 mW/cm^2 curve. As seen from the graph the device has a broad range of optimum performance, where 180° of phase shift results in about 20 dB of insertion loss. This is quite comparable to the losses reported for purely Schottky-controlled CPW phase shifters [25, 27].

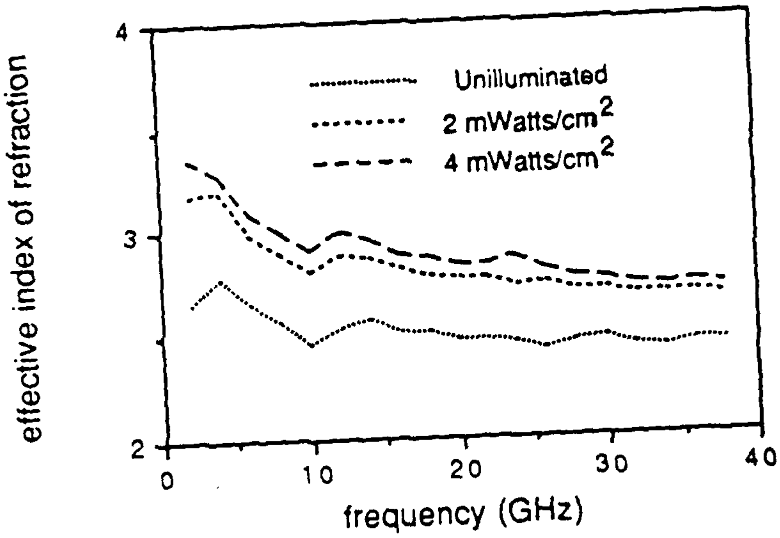

Unilluminated
2 mWatts/cm2
4 mWatts/cm2
effective index of refraction
4
3
2
0
10
20
30
40
frequency (GHz)

Figure 15

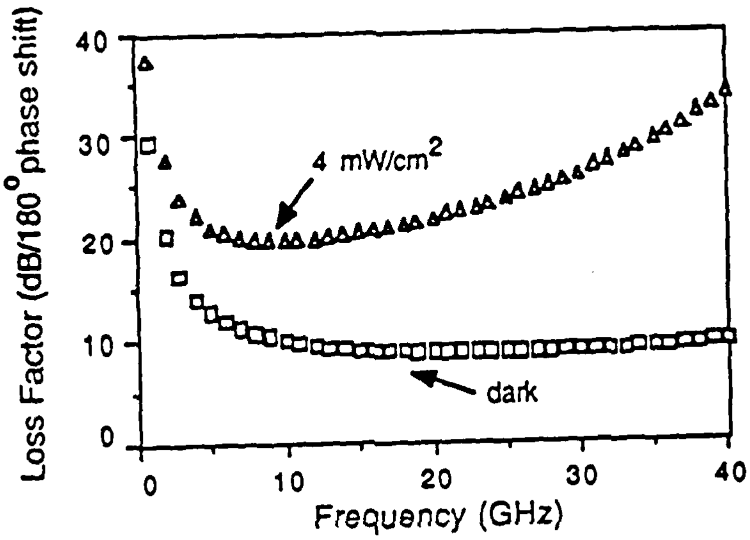
Loss Factor (dB/180°phase shift)
40
30
20
10
0
4 mW/cm2
dark
0
10
20
30
40
Frequency (GHz)

Figure 16

We have also characterized another device which uses a 2 μm thick n-type (1×10^{16} cm^{-3}) epitaxial layer on an SI GaAs substrate for comparison with the device made on the thicker (7 μm) p-type epilayer. For a +6V bias on the center conductor, Fig. 17 shows the insertion loss for the device on the 2 μm thick n-type layer, while the phase shift is given in Fig. 18 and the quality factor is given in Fig. 19. Here the measurements were done at five different illuminating intensities. The maximum illuminating intensity was 2.6 mW/cm^2 and the rest of the illuminating intensities are 1.8mW/cm^2 (-3dB referenced to the maximum intensity), 0.18mW/cm^2 (-13dB), 0.018mW/cm^2 (-23dB), and unilluminated. The results obtained from this device are also very encouraging. For example, at about 20GHz, a phase shift of 125° was obtained for a maximum illuminating intensity of 2.6mW/cm^2. The actual area exposed to the illumination is the same as for the p-type device ($1.4 \times 10^{-3} cm^2$), so the actual absorbed power is only 3.6μW. The optimum operating frequency of the device within the range of values tested is 4GHz. At this frequency the quality factor is about 25dB/180° of phase shift. This result is quite similar to the p-type device, while requiring only 6V of bias, compared to the 35V used with the p-type layer. Figure 20 shows the variation of n_{eff} as a function of optical intensity for three different frequencies, 0.1GHz, 1GHz and 10GHz. Over this range, the change in n_{eff} varied from 12 to 3 over a range of 20dB of optical intensity.

Note that all of the above measurements are done at a reverse bias of +6V. This applied voltage is variable and in fact provides an additional variable to maximize the performance of the phase shifter. This is clearly demonstrated in Fig. 21, which shows the variation of the quality factor for five different applied voltages (+4, +5, +6, and +10V) with the illuminating intensity fixed at 0.018mW/cm^2. The quality factor is optimum at 3GHz for a +6V bias. At +4V, the optimum operating frequency is 0.3GHz and at a higher bias the optimum quality factor moves to a higher frequency.

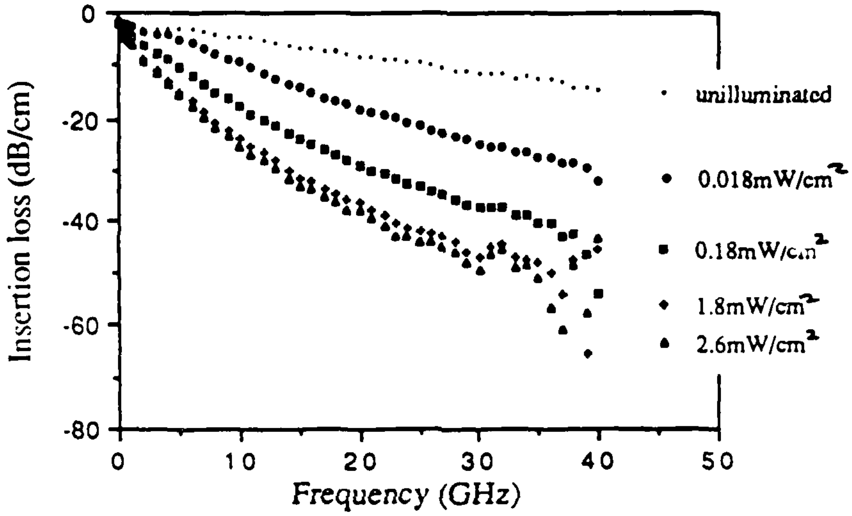

0
-20
-40
-60
-80
0
10
20
30
40
50
Insertion loss (dB/cm)
Frequency (GHz)
unilluminated
0.018mW/cm²
0.18mW/cm²
1.8mW/cm²
2.6mW/cm²

Figure 17

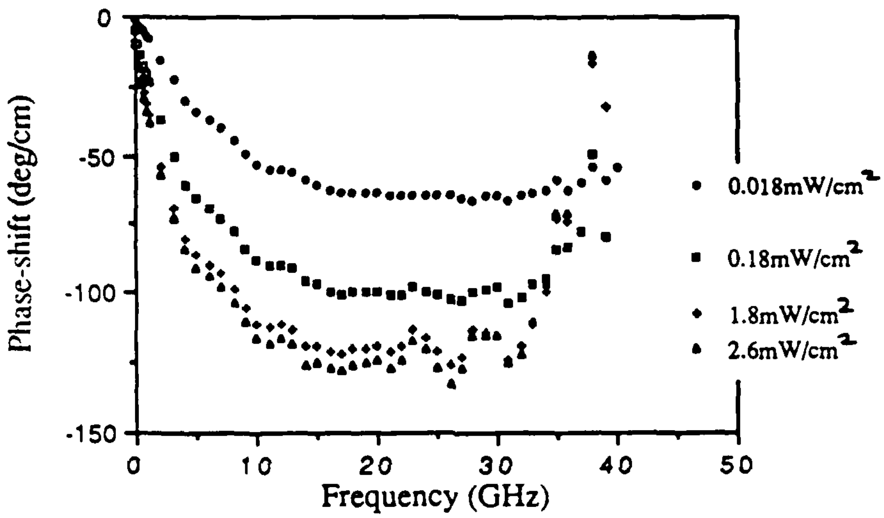

0
-50
-100
-150
Phase-shift (deg/cm)
0
10
20
30
40
50
Frequency (GHz)
0.018mW/cm2
0.18mW/cm2
1.8mW/cm2
2.6mW/cm2

Figure 18

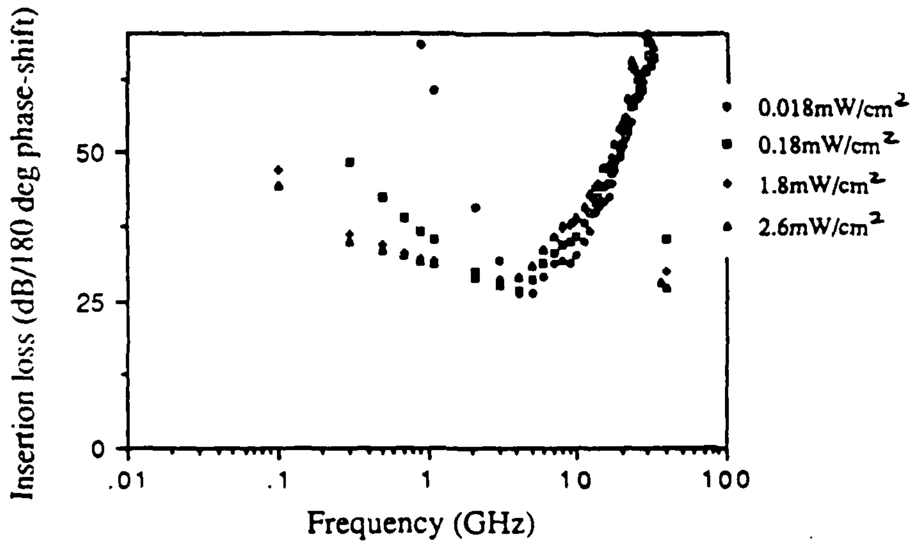
Insertion loss (dB/180 deg phase-shift)
50
25
0
.01
.1
1
10
100
Frequency (GHz)
0.018mW/cm2
0.18mW/cm2
1.8mW/cm2
2.6mW/cm2

Figure 19

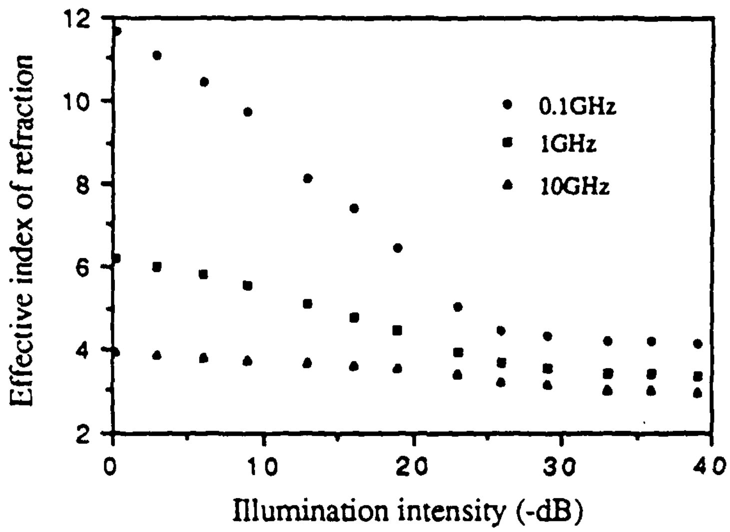

0.1GHz
1GHz
10GHz
Effective index of refraction
Illumination intensity (-dB)
12
10
8
6
4
2
0
10
20
30
40

Figure 20

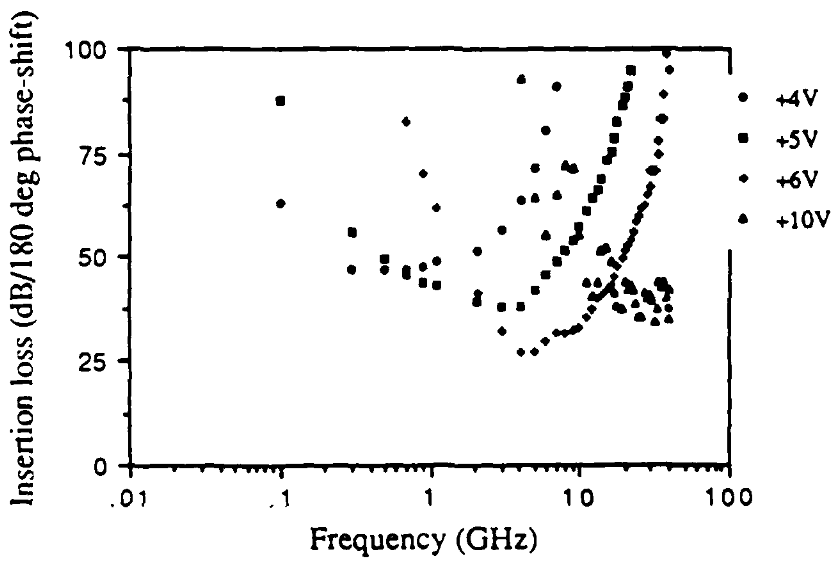
Insertion loss (dB/180 deg phase-shift)
100
75
50
25
0
.01
.1
1
10
100
Frequency (GHz)
+4V
+5V
+6V
+10V

Figure 21

Another important characteristic of a phase shifter is the speed of the device. For distributed CPW devices the control mechanism should play an important role in determining the speed. For a Schottky-controlled device, the high frequency behavior of the bias circuit is probably the practical limitation. In a purely optically controlled device, the speed is dependent on the minority carrier lifetime. Here the trade-off is between fast response (requiring short lifetimes) and efficient generation (which requires long lifetimes). Fast devices would require very intense light sources, while sensitive devices would probably be very slow. The Schottky-contact/optical control approach, however, has the advantage that it is not limited by the bias circuit or directly effected by minority carrier lifetimes. It may be possible to use this approach to achieve both very sensitive control and very high speed phase modulation.

IX. Conclusion

Coplanar waveguide transmission lines on semiconductor substrates, while structurally suited for optical control of the slow-wave factor, will require very high optical illumination intensities to produce useful phase shifts. Thus, this technique is probably not practical for MMIC applications. However, by combining a reverse-biased, Schottky-contacted CPW with controlled optical illumination, large phase shifts at very low intensities have been achieved. The advantages of optical control are thereby preserved, while requiring optical input powers well within the reach of light emitting diodes or low-power diode lasers. A prototype device has produced insertion loss performance comparable to the best results reported to date on Schottky-contact controlled CPW phase shifters.

Since the prototype device has not yet been optimized in terms of dc bias, epitaxial layer thickness or doping concentration, or wavelength of the illuminating source, an optimized Schottky-contacted/optically controlled CPW may be able to achieve significantly better performance. The use of periodic structures may also allow larger phase shifts over narrower bandwidths at very low loss. Even so, the extremely high sensitivity of the current device (at least 20°/cm/μW at 40 GHz) may allow the development of a number of new applications of slow-wave effects in coplanar waveguides.

X. References

1. T. M. Hyltin, "Microstrip transmission on semiconductor dielectric," *IEEE Trans. Microwave Theory Tech.*, vol. MTT-13, pp. 777-781, Nov. 1965.

2. H. Guckel, P. A. Brennen, and I. Palocz, "A parallel plate waveguide approach to microminiaturized, planar transmission lines for integrated-circuit chips," *IEEE Trans. Microwave Theory Tech.*, vol. MTT-15, pp. 468-476, Aug. 1967.

3. I. T. Ho and S. K. Mullick, "Analysis of transmission lines on integrated-circuit chips," *IEEE J. Solid-State Circuits*, vol. SC-2, pp. 201-208, Dec. 1967.

4. H. Hasegawa, M. Furukawa, and H. Yanai, "Properties of microstrip line on Si-SiO_2 system," *IEEE Trans. Microwave Theory Tech.*, vol. MTT-19, pp. 869-881, Nov. 1971.

5. G. M. Hughes and R. M. White, "Microwave Properties of Nonlinear MIS and Schottky-Barrier Microstrip," *IEEE Trans. Electron Devices*, vol. ED-22, pp. 945-955, Oct. 1975.

6. G. M. Hughes, "Electromagnetic slow-wave devices utilizing metal-insulator-semiconductor microstrip, " Ph. D. dissertation, University of California, Berkeley, 1973.

7. Y. Fukuoka and T. Itoh, "Analysis of Slow-Wave phenomena in Coplanar Waveguide on a Semiconductor Substrate, " *Electron. Lett.*, vol.18, pp. 589-590, July 1982.

8. Y. C. Shih and T. Itoh, "Analysis of printed transmission lines for monolithic integrated circuits, " *Electron. Lett.*, vol 18, pp. 585-586, July 1982.

9. P. Kennis, P. Pribetich, Ph. Gelin, M. Aubourg, J. P. Villotte, F. Godon, and Y. Garault, "Properties of Microstrip and Coplanar Lines on Semiconductor Substrates," *Proc. 12th European Microwave Conf.*, Helsinki, pp. 328-333, Sept. 1982.

10. Y. Fukuoka, Yi-Chi Shih, and T. Itoh, "Analysis of Slow-Wave Coplanar Waveguide for Monolithic Integrated Circuits, " *IEEE Trans. Microwave Theory Tech.*, vol. MTT-31, pp. 567-573, July 1983.

11. M. Aubourg, J. P. Villotte, F. Godon, Y. Garault, P. Kennis, P. Prietich, C. Seguinot, and Ph. Gelin, "Analysis of M.I.S. or Schottky Coplanar Lines using the F.E.M. and the S.D.A.," *IEEE MTT-S Int. Microwave Symp. Dig.*, Boston, pp. 396-398, June 1983.

12. R. Sorrentino, G. Leuzzi, and A. Silbermann, "Characteristics of Metal-Insulator-Semiconductor Coplanar Waveguides for Monolithic Microwave Circuits," *IEEE Trans. Microwave Theory Tech.*, vol. MTT-32, pp. 410-416, April 1984.

13. C.-K. Tzuang and T. Itoh, "Finite Element Analysis of Slow-Wave Schottky Contact Printed Line, "*IEEE Trans. Microwave Theory Tech.*, vol. MTT-34, pp. 1483-1490, Dec. 1986.

14. H. Hasegawa and H. Okizaki, "M.I.S. and Schottky slow-wave coplanar striplines on GaAs substrate," *Electron. Lett.*, vol. 13, pp. 663-664, Oct. 1977.

15. Y.R. Kwon, V.M. Hietala, and K. S. Champlin, "Quasi-TEM analysis of 'slow-wave' mode propagation on coplanar microstructure MIS transmission lines," *IEEE Trans. Microwave Theory Tech.*, vol. MTT-35, pp. 545-551, June 1987.

16. C. Seguinot, P. Kennis, and P. Pribetich,"Desktop Computer appraisal of potential slow-wave propagation characteristic for Schottky Coplanar lines," *Electron. Lett.*, vol. 19, pp. 1065-1067, Dec. 1983.

17. M. E. McKaughan and F. C. Jain, "Analysis of a Novel Monolithic GaAs MIS Phase-Shifter," *13th Int. Conf. on Infrared Millimeter Wave Dig.*, pp. 330-331, Dec. 1988.

18. M. E. McKaughan and F. C. Jain, "Quasi-TEM Slow-Wave Analysis of a Monolithic InGaAs/InP Metal-Insulator-Semiconductor Phase-Shifter," *14th Int. Conf. on Infrared and Millimeter Wave Dig.*, pp. 348-349, Dec. 1989.

19. H. Hasegawa and H. Okizaki, "M.I.S. and Schottky slow-wave coplanar striplines on GaAs substrate," *Electron. Lett.*, vol. 13, Oct. 1977, pp. 663-664.

20. R. E. Niedert and C. M. Krowne, "Voltage Variable Microwave Phase Shifter, " *Electron. Lett.*, vol. 21, 1985, pp. 636-638.

21. V. M. Hietala, Y. R. Kwon, and K. S. Champlin, " Broadband Continuously-Variable Phase-Shifter Employing a Distributed Schottky Contact on Silicon," *Electron. Lett.*, vol. 23, 1987, pp 675-677.

22. P. Cheung, D. Fun, D. Miller, C.-K.C. Tzuang, D.P. Neikirk, and T. Itoh, "Optically Controlled Coplanar Waveguide Millimeter Wave Phase Shifter," Tenth International Conference on Infrared and Millimeter Waves, Lake Buena Vista, FL, Dec. 9-13, 1985, pp.303-304.

23. R. E. Niedert and C. M. Krowne, "Voltage Variable Microwave Phase Shifter, " *Electron. Lett.*, vol. 21, pp. 636-638, 1985.

24. C. M. Krowne and R. E. Niedert, "Slow wave monolithic variable phase shifter," *10th Int. Conf. on Infrared and Millimeter Wave Dig.*, pp. 275-276, Dec. 1985.

25. C. M. Krowne and R. E. Niedert,"Slow wave monolithic variable phase shifter with operation into the millimeter wave wavelength regime," *Int. J. Infrared Millimeter Waves*, vol. 7, pp. 715-728, May 1986.

26. C. M. Krowne and E. J. Cukauskas, "GaAs Slow Wave Phase Shifter Characteristics at Cryogenic Temperatures," *IEEE Trans. Electron Dev.*, vol. ED-34, pp. 124-128, Jan. 1987.

27. V. M. Hietala, Y. R. Kwon, and K. S. Champlin, "Broadband Continuously-Variable Phase-Shifter Employing a Distributed Schottky Contact on Silicon," *Electron. Lett.*, vol. 23, pp. 675-677, June 1987.

28. D. R. Singh and K. S. Champlin, "GaAs Travelling Wave Schottky Contact Coplanar Waveguide with Applications to MMIC," *13th Int. Conf. on Infrared Millimeter Wave Dig.*, pp. 288-289, Dec. 1988.

29. C. H. Lee, P. S. Mak, and A. P. DeFonzo,"Optical Control of Millimeter-Waveguides," *IEEE J. Quantum Electron.*, vol. QE-16, pp. 277-288, Mar. 1980.

30. A. M. Vaucher, C. D. Striffler, and C. H. Lee,"Theory of optically controlled millimeter-wave phase shifters," *IEEE Trans. Microwave Theory Tech.*, vol. MTT-31, pp. 209-216, Feb. 1983.

31. M.G. Li, W.L. Cao, V.K. Mathur, and C.H. Lee, "Wide bandwidth high-repetition rate optoelectronic modulation of millimeter waves in GaAs waveguide." *Electron. Lett.*, vol. 14, pp. 454-456, 1982.

32. J. K. Butler, T. F. Wu, and M. W. Scott, "Nonuniform Layer Model of a Millimeter-Wave Phase-Shifter," *IEEE Trans. Microwave Theory Tech.*, vol. MTT-34, pp. 147-155, Jan. 1986.

33. C.-K. Tzuang, P. Cheung, D.P. Neikirk, and T. Itoh, "Analysis of an Optically Controlled CPW Phase Shifter Containing Laterally Non-uniform Lossy Layers," *11th International Conference on Infrared and Millimeter Waves*, Pisa, Italy, pp. 127-129, Dec. 1986.

34. W. Platte and B. Sauerer, "Optically CW-Induced Losses in Semiconductor Coplanar Waveguides," *IEEE Trans. Microwave Theory Tech.*, vol. MTT-37, pp. 139-149, Jan. 1989.

35. R. J. Nelson and R. G. Sobers, "Minority-carrier lifetime and internal quantum efficiency of surface-free GaAs,"*J. Appl Phs.*, vol. 49, pp. 6103-6108, Dec. 1978.

36. M. W. Scott, T. F. Wu, and J. K. Butler, "Analysis of a Buried Layer Millimeter-Wave Phase-Shifter," *IEEE Trans. Microwave Theory Tech.*, vol. MTT-35, pp. 783-784, Aug. 1987.

37. Y.D. Lin, D.P. Neikirk, and T. Itoh, "Coplanar Waveguide Phase Shifter Controlled by a Spatially Periodic Optical Illumination," **Int. J. Infrared and Millimeter Waves 8**, pp. 1027-1036, Sept. 1987.

38. P. R. Herczfeld, A. S. Daryoush, A. Rosen, P. Stabile, and V. M. Contarino, "Optically Controlled Microwave Devices," *RCA Review*, vol. 46, pp. 528-551, Dec. 1985.

39. P. J. Stabile, A. Rosen, and P. R. Herczfeld, "Optically Controlled Lateral PIN Diodes and Microwave Control Circuits," *RCA Review*, vol. 47, pp. 443-456, Dec. 1986.

40. P. R. Herczfeld, A. Poalella, A. S. Daryoush, W. Jemison, and A. Rosen, "Optical Control of MMIC-Based T/R Modules," *Microwave Journal*, pp. 309-321, May 1988.

41. P. Cheung, D. P. Neikirk, and T. Itoh, "Schottky -Biased, Optically Controlled Coplanar Waveguide Phase-Shifter," *Electron. Lett.*, vol.25, pp. 1301-1302, Sept. 1989.

Papers and Conference Presentations Supported in Whole in or in Part by this Grant:

1. "Optically Controlled Coplanar Waveguide Millimeter Wave Phase Shifter," Tenth International Conference on Infrared and Millimeter Waves, p.303, Lake Buena Vista, FL, pp. 303-304, Dec. 9-13, 1985 (P. Cheung, D. Fun, D. Miller, C.-K.C. Tzuang, D.P. Neikirk, and T. Itoh)

2. "Finite element analysis of slow-wave Schottky printed line," 1986 IEEE MTT-S Microwave Symposium Digest, June 2-4, 1986, Baltimore, MD (C-K Tzuang, Q. Zhang and T. Itoh).

3. "Finite Element Analysis of Slow Wave Coplanar Waveguide with Localized Depletion Regions," 16th European Microwave Conference, pp. 471-476, Sept. 8-12, 1986, Dublin, Ireland (C.-K. C. Tzuang and T. Itoh).

4. "Finite Element Analysis of Slow Wave Schottky Contact Printed Lines," IEEE Trans. Microwave Theory and Techniques, Vol. MTT-34, No. 12, December 1986 (C.-K. Tzuang and T. Itoh).

5. "Analysis of an Optically Controlled CPW Phase Shifter Containing Laterally Non-uniform Lossy Layers, Eleventh International Conference on Infrared and Millimeter Waves, pp. 127-129, Pisa, Italy, Dec., 1986 (C.,-K. Tzuang, P. Cheung, D. P. Neikirk, and T. Itoh).

6. "Picosecond Response of an Optically Controlled Millimeter Wave Phase Shifter," Second Topical Meeting on Picosecond Electronics and Optoelectronics, pp. 182-184, Jan., 1987 (C.-K. Tzuang, D. Miller, T.-H. Wang, D. P. Neikirk, T. Itoh, P. Williams, and M. Downer).

7. "High Speed Pulse Transmission Along a Slow-wave CPW for Monolithic Microwave Integrated Circuits," IEEE Trans. Microwave Theory and Techniques, Vol. MTT-35, August 1987 (C.-K. Tzuang and T. Itoh).

8. "Coplanar Waveguide Phase Shifter Controlled by a Spatially Periodic Optical Illumination," Int. J. Infrared and Millimeter Waves Vol. 8, pp. 1027-1036, Sept. 1987 (Y.D. Lin, D.P. Neikirk, and T. Itoh).

9. "Periodically Illuminated CPW Phase Shifter," 12th International Conference on Infrared and Millimeter Waves, pp. 93-94, Dec. 14-18, 1987 (Y.-D. Lin, D.P. Neikirk, and T. Itoh).

10. "Measurements of an Optically Controlled Coplanar Waveguide Phase Shifter," 12th International Conference on Infrared and Millimeter Waves, pp. 91-92, Dec. 14-18, 1987 (P. Cheung, D.P. Neikirk, and T. Itoh)..

11. "Experimental Performance of a Periodically Illuminated Optically Controlled Coplanar Waveguide Phase Shifter," 13th International Conference on Infrared and Millimeter Waves, R.J. Temkin, Editor, SPIE Vol. 1039, Dec. 5-9, 1988, pp. 63-64 (.P. Cheung, D.P. Neikirk, and T. Itoh)

12. "An Optically Controlled Coplanar Waveguide Phase Shifter," IEEE MTT-S International Microwave Symposium Digest, Vol. 1, June 13-15, 1989, pp. 307-309 (P Cheung, D.P. Neikirk, and T. Itoh).

13. "Optically Controlled Coplanar Waveguide Phase Shifters," **Microwave Journal**, Dec. 1989 (D.P. Neikirk, P. Cheung, M.S. Islam, and T. Itoh).

14. "A Schottky-Biased, Optically-Controlled Coplanar Waveguide Phase Shifter," **Electronics Letters 25**, Sept. 14, 1989, pp. 1301-1302 (P. Cheung, D.P. Neikirk, and T. Itoh).

15. "Measurements of an Optically Controlled Coplanar-Waveguide Phase-Shifter," to be presented at MIOP 90, April 24-26, 1990, Stuttgart, West Germany.

16. "Optically Controlled Coplanar Waveguide Phase-Shifters," to be published in IEEE Trans. Microwave Theory and Techniques, 1990 (P. Cheung, D.P. Neikirk, and T. Itoh).

Technical Interactions and Oral Presentations at Seminars and Conferences

D.P. Neikirk, "Optically Controlled Coplanar Waveguide Millimeter Wave Phase Shifter," Tenth International Conference on Infrared and Millimeter Waves, Lake Buena Vista, FL, Dec. 9-13, 1985.

D. P. Neikirk, "Exotic Heterojunction Devices for Microwave Circuits," NSF Workshop on Future Research Opportunities in Electromagnetics, Arlington, TX, January 29-31, 1986.

D.P. Neikirk, "Optical Control of a Monolithic Millimeter Phase Shifter," ARO Workshop on Fundamental Issues in Millimeter and Submillimeter Waves, Los Angeles, Ca., Sept. 15-16, 1986.

T. Itoh, presentation at ARO Workshop on Fundamental Issues in Millimeter and Submillimeter Waves, Los Angeles, Ca., Sept. 15-16, 1986.

T. Itoh, presentation at DoD Symposium on Millimeter Wave/Microwave Measurements and Standards, Redstone Arsenal, Huntsville, Alabama, November 6-7, 1986.

D. P. Neikirk, "Picosecond Responses of an Optically Controlled Millimeter Wave Phase Shifter," Topical Meeting on Picosecond Electronics and Optoelectronics, Lake Tahoe, NV, (January 14-16, 1987).

P. Cheung, "Experimental Performance of an Optically Controlled Coplanar Waveguide Phase Shifter," 12th International Conference on Infrared and Millimeter Waves, Lake Buena Vista, FL, (Dec. 14-18, 1987).

D. P. Neikirk, "Periodically Illuminated CPW Phase Shifter," 12th International Conference on Infrared and Millimeter Waves, Lake Buena Vista, FL, (Dec. 14-18, 1987).

P Cheung, "An Optically Controlled Coplanar Waveguide Phase Shifter," IEEE MTT-S International Microwave Symposium, Long Beach, CA, (June 13-15, 1989).

T. Itoh, "Measurements of an Optically Controlled Coplanar-Waveguide Phase-Shifter," to be presented at MIOP 90, Stuttgart, West Germany (April 24-26, 1990).

Technical Reports

1. "Finite Element Analysis of Slow-Wave Schottky Contact Printed Lines," Microwave Laboratory Report No. 87-P-2, AFOSR Grant 86-0036, Feb. 16, 1987, (C-K Tzuang, D. P. Neikirk, and T. Itoh).

2. "Annual Technical Report on Monolithic Phase Shifter Study", Microwave Laboratory Report No. 87-P-3, AFOSR Grant 86-0036, Feb. 23, 1987, (D. P. Neikirk and T. Itoh).

3. "Complex modes in lossless shielded guiding structures," Microwave Laboratory Report No. 87-P-6, AFOSR Grant 86-0036, May 1987, (W.-X. Huang and T. Itoh).

4. "Annual Technical Report on Monolithic Phase Shifter Study", Microwave Laboratory Report No. 87-P-10, AFOSR Grant 86-0036, Nov. 25, 1987, (D. P. Neikirk and T. Itoh).

5. "Final Technical Report on Monolithic Phase Shifter Study", Microwave Laboratory Report No. 90-P-1, AFOSR Grant 86-0036, Feb. 15, 1990, (D. P. Neikirk and T. Itoh).

Participating Professionals and Advanced Degrees Awarded

Dean P. Neikirk, Associate Professor, UT Austin
T. Itoh, Professor, UT Austin

C-K Tzuang, UT Austin, PhD awarded: December, 1986, "Slow-wave propagation on monolithic microwave integrated circuits with layered and non-layered structures."

Yu-De Lin, UT Austin, M.S. awarded: May 1987, "Metal-Insulator-Semiconductor and Optically Controlled Slow-Wave Structures."

P. Cheung, UT Austin, MS awarded: December, 1987, "A preliminary study of an optically controlled coplanar waveguide phase shifter."

W.-X. Huang, UT Austin, MS awarded: May, 1989, "Complex modes in lossless shielded guiding structures."

P. Cheung, UT Austin, PhD to be awarded: May, 1990, "Optically controlled coplanar waveguide phase shifters."

Consultative and Advisory Functions

T. Itoh has been on the Committee on Army Basic Research for National Research Council.

T. Itoh participated in the U.S. Army Electronics Research Strategy Workshop held at Quail Roost, NC on May 3-6, 1987 as an invited speaker and a panel member to identify millimeter-wave and electromagnetic research areas important to the Army.

On July 13-15, 1987, T. Itoh participated in a DARPA Workshop on Electromagnetic Simulations, Packaging and Measurements of High-Speed Devices organized by the Materials Research Council. Prof. Itoh presented an invited talk on, "2D and 3D Electromagnetic Models at Frequencies above 5 GHz."

Professors Itoh, Neikirk and Streetman were visited by Dr. D. Arndt from NASA Johnson Space Center on November 13, 1987 to discuss microwave and millimeter-wave integrated circuit research.